Solid-State Electronics, 1977, Vol. 20, pp. 753–771. Pergamon Press. Printed in Great Britain

AN ANALYTICAL MODEL FOR THE EPITAXIAL BIPOLAR TRANSISTOR

B. L. GRUNG and R. M. WARNER, JR.
Department of Electrical Engineering, University of Minnesota, Minneapolis, MN 55455, U.S.A.

(*Received* 15 *October* 1976; *in revised form* 9 *March* 1977)

Abstract—In the $n^+pn^-n^+$ transistor, high-current effects in the base and collector regions are linked within the current ranges of practical interest. To describe such effects, we have derived an analytical model that is based primarily on five assumptions: (1) the structure is approximately one-dimensional; (2) recombination is negligible in the base and collector quasi-neutral regions, and in the three space-charge regions; (3) high-current effects are negligible in the emitter and n^+-substrate regions; (4) the Fletcher boundary conditions (or the Misawa boundary conditions) can be used for the three space-charge regions; and (5) the ambipolar approach can be used for the base and collector quasi-neutral regions. The primary findings predicted by the $n^+pn^-n^+$ transistor model are: In current ranges of practical interest (usable current gain), the electron concentration profile has a significant "vertical step" located at the collector-base metallurgical junction for all values of collector current. In the limit of extremely-high-current operation, this step tends to vanish. In the current range where the current gain begins to decline rapidly with increasing collector current, the electron concentration at the base boundary of the collector-base space-charge region goes approximately as the square of the hole concentration at the collector boundary of the same region. Because of this relationship, a charge-control calculation is more difficult than a straightforward calculation of carrier concentration for a given degree of accuracy. The $n^+pn^-n^+$ transistor model (which consists of twelve algebraic equations) is particularly useful for the practically important case of an epitaxial bipolar transistor having a very thin, heavily-doped base region.

NOTATION

A_E surface area of the emitter region, cm^2
$b_B(b_C)$ defined as $\mu_{nB}/\mu_{pB}(\mu_{nC}/\mu_{pC})$
$D_n(D_p)$ electron (hole) diffusion constant, cm^2/sec
D_{nB}, etc. average electron diffusion constant in the base region, etc., cm^2/sec
$E(x)$ electric field, V/cm
I_B base current, A
I_C collector current, A
$I_n(x)$ electron current, A
$I_p(x)$ hole current, A
$I_n(x_{\epsilon B})$, etc. electron current at the boundary between the emitter-base space-charge region and the active-base region, etc., A
$J_n(x)$, etc. electron current density, etc., A/cm^2
$J(x)$ total current density, which is defined as $J_p(x)+J_n(x)$, A/cm^2
h_{fe} the a.c. current gain
(kT/q) thermal voltage, V
$L_n(L_p)$ electron (hole) diffusion length, cm
L_{nE}, etc. average electron diffusion length in the emitter region, etc., cm
$N_A(N_D)$ acceptor (donor) impurity concentration, cm^{-3}
N_{AB}, etc. average acceptor impurity concentration in the base region, etc., cm^{-3}
n_i intrinsic concentration of holes or electrons, cm^{-3}
n_{iE} effective intrinsic concentration of holes or electrons in the emitter region, cm^{-3}
$n_0(p_0)$ equilibrium electron (hole) concentration, cm^{-3}
n_{0B}, etc. average equilibrium electron concentration in the base region, etc., cm^{-3}
$n(x)$ electron concentration, cm^{-3}
$p(x)$ hole concentration, cm^{-3}
$n(x_{\epsilon B})$, etc. electron concentration at the boundary between the emitter-base space-charge region and the active-base region, etc., cm^{-3}
q electronic charge, coul
$Q_{B0}(Q_{C0})$ equilibrium base (collector) charge, coul
$Q_B^*(Q_C^*)$ stored minority carrier charge in the active base (quasi-neutral collector) region, coul
R_{0B} series resistance of the inactive base region, ohms
r_0 small-signal output resistance in the common-emitter configuration, ohms
T absolute temperature, °K
V_{CB} collector-base (terminal) voltage, V
V_{EB} emitter-base (terminal) voltage, V
V_{jC}, etc electrostatic potential drop across the collector-base space-charge region minus the corresponding potential drop at equilibrium, etc., V
X_B, etc. thickness of the active-base region, etc., cm
x distance measured from the silicon surface, cm
$x_{\epsilon B}$, etc. distance value which locates the boundary between the emitter-base space-charge region and the active-base region, etc., cm
x_{jE}, etc. distance value which locates the metallurgical boundary between the emitter and base regions, etc., cm
y distance measured laterally from the center of the active-base region, cm
β_F the d.c. current gain
$\gamma(x)$ defined as $J_p(x)/J(x)$
γ_C average value of $J_p(x)/J(x)$ in the collector region
$\Delta\phi_{jE}$, etc. defined as $\phi_n(x_{\epsilon E})-\phi_p(x_{\epsilon B})$, etc., V
ϵ dielectric constant, farad/cm
$\mu_n(\mu_p)$ electron (hole) mobility, cm^2/(V sec)
μ_{nB}, etc. average electron mobility in the base region, etc., cm^2/(V sec)
ξ_1, etc. see Section 5
$\rho(x)$ source density, coul
$\phi_n(x)$ electron quasi-Fermi potential, V
$\phi_p(x)$ hole quasi-Fermi potential, V
$\psi(x)$ electrostatic potential, V
$\psi_0(x)$ electrostatic potential for equilibrium conditions, V
ψ_{0C}, etc. built-in voltage of the collector-base junction, etc., V.

Greek subscripts: These subscripts are to indicate that the value of the x variable locates the boundary between space-charge and quasi-neutral regions. The various Greek subscripts are matched with space-charge regions as follows: emitter-base junction, ϵ; collector-base junction, γ; high-low junction, η; and pn junction, μ.

1. INTRODUCTION

An analytical model for the epitaxial bipolar transistor is derived here. At low currents, this model is completely consistent with the Ebers-Moll model[1]; at high currents, it is nearly consistent with the Gummel-Poon model[2]. For small base thicknesses ($X_B < 1\,\mu$m), it describes high-current phenomena—notably, the Kirk effect[3] and the Webster effect[4]—more accurately than the Gummel-Poon model does.

To derive the analytical model, we divide the epitaxial bipolar transistor, which is called here the $n^+pn^-n^+$ transistor, into space-charge and quasi-neutral regions. The Fletcher boundary conditions[5] are then used for each space-charge region. And the ambipolar approach is employed for each quasi-neutral region. The ambipolar approach, which has its roots in plasma theory, was first used extensively for semiconductor problems by van Roosbroeck[6]. Van Vliet[7] has examined critically the use of this approach for the *pn* diode; more recently, van Vliet and Min[8] have employed the ambipolar approach to derive an analytical model for a p^+np^+ transistor. Some equations of the present paper resemble those of van Vliet and Min. Other equations are closely related to those derived by Beale and Slatter[9] and by Pals and de Graaff[10].

The $n^+pn^-n^+$ transistor model is given at the end of this paper. The simpler model for an idealized n^+pn^- transistor is first derived. This transistor has: (1) electron current patterns that allow the use of one-dimensional equations, and (2) metallurgical regions that are uniformly doped. The n^+pn^- transistor model is then examined quantatively for one specific structure wherein (1) the emitter region is heavily doped ($N_{DC} = 10^{20}\,\text{cm}^{-3}$), (2) the base region is moderately doped ($N_{AB} = 10^{17}\,\text{cm}^{-3}$) and has an active portion $0.5\,\mu$m thick, and (3) the collector region is lightly doped ($N_{DC} = 2\times10^{15}\,\text{cm}^{-3}$) and is $15\,\mu$m thick.

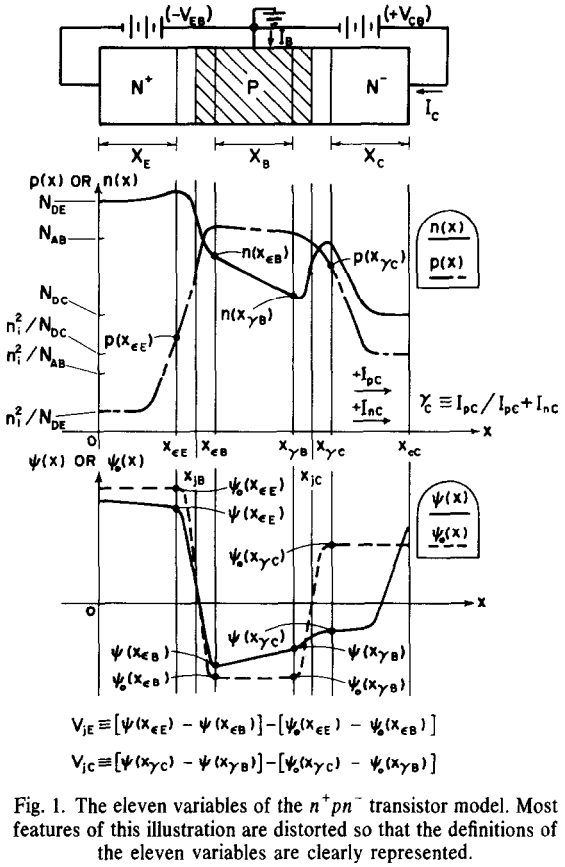

Fig. 1. The eleven variables of the n^+pn^- transistor model. Most features of this illustration are distorted so that the definitions of the eleven variables are clearly represented.

The n^+pn^- transistor model consists of nine equations that contain eleven variables which are defined in Fig. 1 above. Four of the variables (V_{EB}, V_{CB}, I_C and I_B) are termed the "external" variables since they can be directly measured at the terminals. The remaining seven "internal" variables are: $p(x_{\epsilon E})$, $n(x_{\epsilon B})$, $n(x_{\gamma B})$, $p(x_{\gamma C})$, V_{jE}, V_{jC} and γ_C. The first four internal variables represent the minority carrier concentrations at the four boundaries of the two space-charge regions. These boundaries, which are located at the positions $x_{\epsilon E}$, $x_{\epsilon B}$, $x_{\gamma B}$ and $x_{\gamma C}$, are assumed to be fixed. The emitter-base junction voltage V_{jE} is defined as the electrostatic potential drop across the emitter-base space-charge region minus the corresponding potential drop at equilibrium. The collector-base junction voltage V_{jC} is defined in a similar way. The last internal variable γ_C is defined as the ratio of the hole current $I_p(x_{\gamma C})$ to the total current $[I_p(x_{\gamma C}) + I_n(x_{\gamma C})]$.

In the next section, the n^+pn^- transistor model is derived. For convenience, the nine equations that make up this model are summarized here:

$$p(x_{\epsilon E}) = \frac{n_{iE}^2}{N_{DE}}\left(\exp\frac{q(-V_{jE})}{kT}\right)\left[1+\left(\frac{n_i}{N_{AB}}\right)^2\left(\exp\frac{q(-V_{jE})}{kT}\right)\right] \tag{1}$$

$$n(x_{\epsilon B}) = \frac{n_i^2}{N_{AB}}\left(\exp\frac{q(-V_{jE})}{kT}\right) \tag{2}$$

$$n(x_{\gamma B}) = \frac{n_i^2}{N_{AB}}\left(\exp\frac{q(-V_{jC})}{kT}\right)\left[\frac{1+\left(\frac{n_i}{N_{DC}}\right)^2\left(\exp\frac{q(-V_{jC})}{kT}\right)}{1-\left(\frac{n_i}{N_{AB}}\right)^2\left(\frac{n_i}{N_{DC}}\right)^2\left(\exp\frac{q(-V_{jC})}{kT}\right)^2}\right] \tag{3}$$

$$p(x_{\gamma C}) = \frac{n_i^2}{N_{DC}}\left(\exp\frac{q(-V_{jC})}{kT}\right)\left[\frac{1+\left(\frac{n_i}{N_{AB}}\right)^2\left(\exp\frac{q(-V_{jC})}{kT}\right)}{1-\left(\frac{n_i}{N_{AB}}\right)^2\left(\frac{n_i}{N_{DC}}\right)^2\left(\exp\frac{q(-V_{jC})}{kT}\right)^2}\right] \tag{4}$$

$$I_B + \gamma_C I_C = qA_E\frac{D_{pE}}{L_{pE}}\left[p(x_{\epsilon E}) - \frac{n_{iE}^2}{N_{DE}}\right] \tag{5}$$

$$I_C(1-\gamma_C) = qA_E\frac{D_{nB}}{X_B}\left\{2[n(x_{\epsilon B}) - n(x_{\gamma B})] - N_{AB}\ln\left[\frac{n(x_{\epsilon B})+N_{AB}}{n(x_{\gamma B})+N_{AB}}\right]\right\} \tag{6}$$

$$V_{EB} = V_{jE} - \frac{kT}{q} \ln\left[1 + \frac{n(x_{\epsilon B})}{N_{AB}}\right] \tag{7}$$

$$I_C = qA_E \frac{D_{nC}}{X_C} \frac{1}{[1-\gamma_C(b_C+1)]} \left\{2\left[p(x_{\gamma C}) - \frac{n_i^2}{N_{DC}}\right] + N_{DC}\left[\frac{1+\gamma_C(b_C-1)}{1-\gamma_C(b_C+1)}\right] \ln\left[\frac{p(x_{\gamma C})[1-\gamma_C(b_c+1)] - \gamma_C b_C N_{DC}}{(n_i^2/N_{DC})[1-\gamma_C(b_C+1)] - \gamma_C b_C N_{DC}}\right]\right\} \tag{8}$$

$$V_{CB} = V_{jC} + \frac{kT}{q}\left[\frac{1+\gamma_C(b_C-1)}{1-\gamma_C(b_C+1)}\right] \ln\left[\frac{p(x_{\gamma C})[1-\gamma_C(b_C+1)] - \gamma_C b_C N_{DC}}{(n_i^2/N_{DC})[1-\gamma_C(b_C+1)] - \gamma_C b_C N_{DC}}\right]. \tag{9}$$

As will be shown, these nine equations predict the major electrical characteristics of the n^+pn^- transistor provided that the collector current I_C is less than a certain critical current I_3. The four operating regimes of the n^+pn^- transistor are defined in Fig. 2. Most numerical calculations given in this paper are associated with the shaded portion of the quasi-saturation regime. Many of the unique characteristics of the n^+pn^- transistor are most conspicuous in this regime.

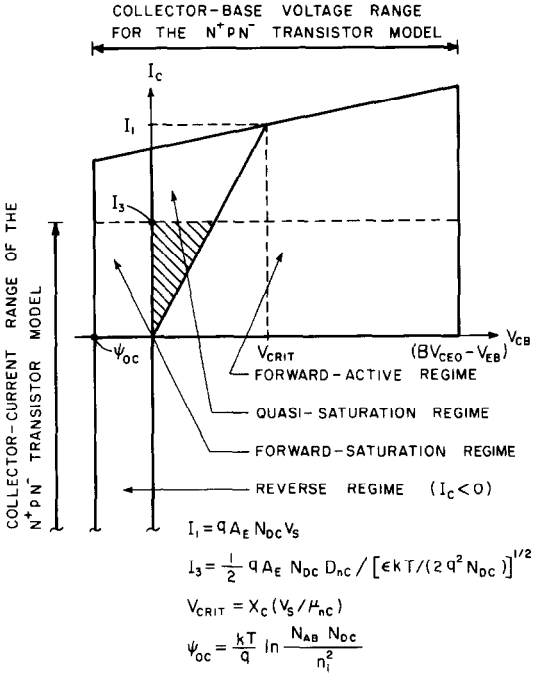

Fig. 2. The four regimes of operation. This illustration employs the collector-base voltage as a variable even though the n^+pn^- transistor is operating in a common-emitter configuration. Regimes are divided by solid lines.

2. DERIVATION OF THE n^+pn^- TRANSISTOR MODEL

The minority-carrier Fletcher boundary conditions for a *pn* diode are

$$p(x_{\mu N}) = \frac{(p_{0P} - n_{0P})p_{0N}n_{0N}\left[\exp\frac{q(-V_j)}{kT}\right] + n_{0P}p_{0N}(n_{0N} - p_{0N})\left[\exp\frac{q(-V_j)}{kT}\right]^2}{p_{0P}n_{0N} - n_{0P}p_{0N}\left[\exp\frac{q(-V_j)}{kT}\right]^2} \tag{10}$$

$$n(x_{\mu P}) = \frac{(n_{0N} - p_{0N})n_{0P}p_{0P}\left[\exp\frac{q(-V_j)}{kT}\right] + p_{0N}n_{0P}(p_{0P} - n_{0P})\left[\exp\frac{q(-V_j)}{kT}\right]^2}{n_{0N}p_{0P} - p_{0N}n_{0P}\left[\exp\frac{q(-V_j)}{kT}\right]^2} \tag{11}$$

where the forms of these equations are similar to those given by van Vliet[7] and where the notation in row one of Table 1 is employed. The Fletcher boundary conditions have been critically examined by several authors[11–18] and the limitations of these relations are well established. Those who are unfamiliar with the subject can profit by reading Hauser's article[16] first. Briefly, the Fletcher boundary conditions are derived from the conventional semiconductor transport equations by the integration of these equations through the space-charge region and from the requirement that the resulting equations must satisfy the condition of electrical neutrality at each of the two boundaries of the space-charge region. The validity of eqns (10) and (11) for a *pn* diode is assumed without further proof.

Table 1. Notation for the *pn* junction, and the emitter-base and collector-base junctions of the n^+pn^- transistor

pn DIODE SPACE-CHARGE REGION	$p(x_{\mu N})$	$n(x_{\mu P})$	$(-V_j)$	n_{0N}	p_{0N}	n_{0P}	p_{0P}
EMITTER-BASE SPACE-CHARGE REGION	$p(x_{\epsilon E})$	$n(x_{\epsilon B})$	$(-V_{jE})$	n_{0E}	p_{0E}	n_{0B}	p_{0B}
COLLECTOR-BASE SPACE-CHARGE REGION	$p(x_{\gamma C})$	$n(x_{\gamma B})$	$(-V_{jC})$	n_{0C}	p_{0C}	n_{0B}	p_{0B}
VAN VLIET'S NOTATION	p_i	n_i^*	V	n_0	p_0	n_0^*	p_0^*

For the emitter-base diode of the n^+pn^- transistor, eqns (10) and (11) become

$$p(x_{\epsilon E}) = \frac{n_{iE}^2}{N_{DE}}\left(\exp\frac{q(-V_{jE})}{kT}\right)\left[\frac{1+\left(\frac{n_i}{N_{AB}}\right)^2\left(\exp\frac{q(-V_{jE})}{kT}\right)}{1-\left(\frac{n_{iE}}{N_{DE}}\right)^2\left(\frac{n_i}{N_{AB}}\right)^2\left(\exp\frac{q(-V_{jE})}{kT}\right)^2}\right] \tag{12}$$

$$n(x_{\epsilon B}) = \frac{n_i^2}{N_{AB}}\left(\exp\frac{q(-V_{jE})}{kT}\right)\left[\frac{1+\left(\frac{n_{iE}}{N_{DE}}\right)^2\left(\exp\frac{q(-V_{jE})}{kT}\right)}{1-\left(\frac{n_{iE}}{N_{DE}}\right)^2\left(\frac{n_i}{N_{AB}}\right)^2\left(\exp\frac{q(-V_{jE})}{kT}\right)^2}\right] \tag{13}$$

if the notations given in row two of Table 1 are used, and if the approximations corresponding to groups A and B of Table 2 are employed. The "effective" intrinsic carrier

Table 2. Approximations for the n^+pn^- transistor†

$N_{DE} \gg n_{iE}$	$N_{AB} > N_{DC}$	$N_{DC} \gg n_i$	GROUP A
$X_E \gg L_{pE}$	$X_B \ll L_{nB}$	$X_C \ll L_{pC}$	
$n_{OE} \approx N_{DE}$	$n_{OB} \approx \frac{n_i^2}{N_{AB}}$	$n_{OC} \approx N_{DC}$	GROUP B
$p_{OE} \approx \frac{n_{iE}^2}{N_{DE}}$	$p_{OB} \approx N_{AB}$	$p_{OC} \approx \frac{n_i^2}{N_{DC}}$	
$\left[\frac{n_{iE}}{N_{DE}}\right]^2 \left[\frac{n_i}{N_{AB}}\right]^2 \left[\exp \frac{q(-V_{jE})}{kT}\right]^2 \ll 1$		$N_{DE} \gg N_{AB}$	GROUP C
$p(x_{\epsilon E}) \gg \frac{n_{iE}^2}{N_{OE}}$	$I_B \gg \gamma_C I_C$	$p(x_{\gamma C}) \gg \frac{n_i^2}{N_{OC}}$	GROUP D
$\left[\exp \frac{q(-V_{jE})}{kT}\right] \gg 1$	$\gamma_C(b_C+1) \ll 1$	$\left[\exp \frac{q(-V_{jC})}{kT}\right] \gg 1$	

†The first row of Group A defines the basic relations among the doping concentrations of three regions of the n^+pn^- transistor. The second row of Group A indicates that recombination is important in the emitter region but is negligible in the base and collector regions. Group B gives the approximate equilibrium hole and electron concentrations of the various regions. Group C states that high-level effects in the emitter region are negligible. Group D is used for the abridged model only.

concentration n_{iE} introduced by de Man[19] is used for the emitter region (see also Martens *et al.*[20]). This constant which accounts for the influence of heavy-doping effects in the emitter region will be set equal to n_i for simplicity in the subsequent numerical calculations. Equations (1) and (2) of the n^+pn^- transistor model result directly from eqns (12) and (13) provided that the two approximations given in group C of Table 2 are used. Together, these two approximations imply that $n(x_{\epsilon B}) \ll N_{DE}$.

Equations (3) and (4) for the collector-base diode are derived directly from eqns (10) and (11) by substituting the notation given in row three of Table 1 and incorporating approximations given in groups A and B of Table 2. The fact that the Fletcher boundary conditions apply for the collector-base diode is not obvious. Consider the n^+pn^- transistor operating in the quasi-saturation regime. Unlike the emitter-base diode which is forward biased externally ($V_{EB} < 0$), the collector-base diode is reverse biased externally ($V_{CB} > 0$). In addition, the direction of the total current through the collector-base diode is opposite to the direction of the current when this diode is externally forward biased. The primary reason that the Fletcher boundary conditions are applicable is that these relations are independent of the current passing through the collector-base space-charge region. The upper current limit for the validity of the Fletcher boundary conditions has been discussed by Hauser[16] and van der Ziel[17] for the *pn* diode. Similar arguments for the collector-base diode of the n^+pn^- transistor can be used to justify the employment of the Fletcher boundary conditions for this diode even at relatively high currents (i.e. currents at which the quasi-neutral regions adjacent to collector-base space-charge region are highly conductivity modulated). Thus, in summary, the Fletcher boundary conditions, which were originally derived for a forward-biased *pn* diode, apply directly to the collector-base diode of an n^+pn^- transistor even when this diode is externally reverse biased ($V_{CB} > 0$).

Because of the extreme-doping approximation ($N_{DE} \gg N_{AB}$) and because of the assumption that recombination dominates behavior in the emitter region ($L_{pE} \ll X_E$), the hole current into the emitter region is given by the expression

$$I_p(x_{\epsilon E}) = -qA_E \frac{D_{pE}}{L_{pE}} \left[p(x_{\epsilon E}) - \frac{n_{iE}^2}{N_{DE}} \right]. \tag{14}$$

When $V_{CB} > 0$, this current results from holes that are supplied from not only the base contact but also the collector contact. The hole and electron flow patterns for the n^+pn^- transistor operating in the quasi-saturation regime are indicated in Fig. 3(a) where it is shown that the hole current $-I_p(x_{\epsilon E})$ into the emitter region is given by

$$-I_p(x_{\epsilon E}) = I_B + \gamma_C I_C. \tag{15}$$

The substitution of eqn (15) into eqn (14) gives eqn (5). The corresponding current patterns for operation in the forward-saturation regime are indicated in Fig. 3(b). By definition, the transistor is operating in this regime when

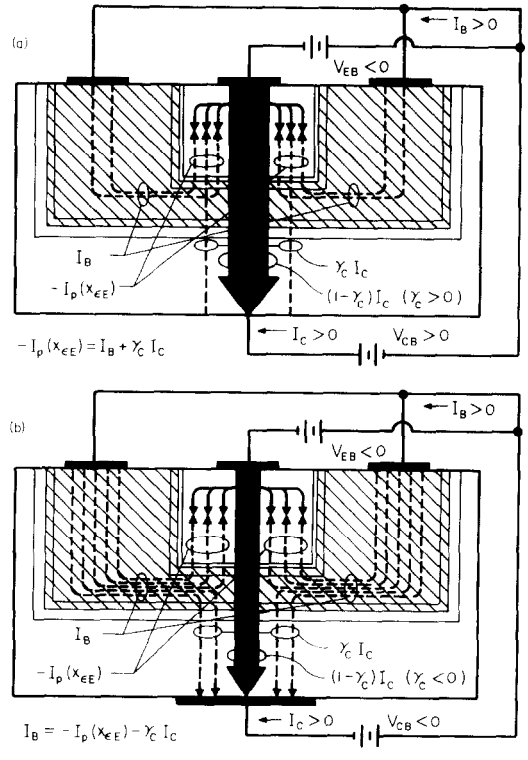

Fig. 3. The hole (dashed lines) and electron (solid lines) particle current patterns. For the upper part, the n^+pn^- transistor is operating in the quasi-saturation regime; for the lower part, it is operating in the forward-saturation regime.

both of its junctions are forward biased externally ($V_{EB}<0$ and $V_{CB}<0$) and when the collector current I_C is positive. For these two conditions, the hole current into the emitter region is again given by eqn (15) as shown in Fig. 3(b), where γ_C is negative.

If the hole current in the base region is negligible compared to the electron current, then the conventional expression for the active base region is applicable (e.g. see Rittner[21]). This expression (which is used for all numerical calculations in the quasi-saturation regime) is

$$I_C = qA_E\frac{D_{nB}}{X_B}\left\{2[n(x_{\epsilon B})-n(x_{\gamma B})] - N_{AB}\ln\left[\frac{n(x_{\epsilon B})+N_{AB}}{n(x_{\gamma B})+N_{AB}}\right]\right\}. \quad (16)$$

Equation (6) of the n^+pn^- transistor model is obtained from eqn (16) by the replacement of I_C by $I_C(1-\gamma_C)$. This modification extends the current range for which the model is valid.

Equation (7) for the emitter-base voltage of the n^+pn^- transistor is derived by an approach that is closely related to the derivation given by van Vliet and Min[8] for the corresponding voltage in a p^+pn^+ transistor. Because of this relationship, the following derivation is brief. The article by van Vliet and Min should be consulted for the details that are lacking here. Since some of the two-dimensional properties of the n^+pn^- transistor must be carefully considered, the structure shown in Fig. 4 is more realistic for this purpose than the original structure shown in Fig. 1. The emitter-base voltage is given by

$$V_{EB} = V_{jE} + [\psi(x_{\epsilon B}, y_1) - \psi(0, y_3)] \quad (17)$$

where $\psi(x_{\epsilon B}, y_1)$ is the value of the potential $\psi(x, y)$ at the point $(x_{\epsilon B}, y_1)$ and $\psi(0, y_3)$ is the corresponding value at the point $(0, y_3)$. Thus, the second term in eqn (17) is the series potential drop measured between these two points. The first point is located on the boundary between active base region and the emitter-base space-charge region. The second point is located on the boundary between the inactive base region and the base ohmic contact.

The series potential drop is found by integration of the electric field $\vec{E}(x, y)$ along the path indicated in the figure. The electric field is given by

$$\vec{E}(x,y) = -\frac{kT}{q}\left(\frac{b_B-1}{b_B+1}\right) \nabla\{\ln[n(x,y)(b_B+1)+(p_{0B}-n_{0B})]\} + \frac{\vec{J}(x,y)}{q\mu_{pB}[n(x,y)(b_B+1)+(p_{0B}-n_{0B})]}. \quad (18)$$

The integration of the first term for the entire path from point $(x_{\epsilon B}, y_1)$ to point $(0, y_3)$ gives the "ambipolar-diffusion" voltage

$$V_{AD} = -\frac{kT}{q}\left(\frac{b_B-1}{b_B+1}\right)\ln\left[\frac{n(x_{\epsilon B}, y_1)(b_B+1)+(p_{0B}-n_{0B})}{p_{0B}+b_Bn_{0B}}\right]. \quad (19)$$

The corresponding integration for the second term of eqn (18) must be divided into three parts. Along the portion of the path between point $(x_{\epsilon B}, y_1)$ and point $(x_{\gamma B}, y_1)$, the hole current density $\vec{J}(x, y)$ is given by

$$\vec{J}(x,y) = +qD_{nB}\left[\frac{2n(x,y)+(p_{0B}-n_{0B})}{n(x,y)+(p_{0B}-n_{0B})}\right]\nabla n. \quad (20)$$

Van Vliet and Min make the unnecessary approximation that $\vec{J}(x, y) = +2qD_{nB}\nabla n$. Such an approximation does not introduce significant errors for typical bias conditions, but it does introduce minor errors for equilibrium conditions. With eqn (20), the integration of the second term in eqn (18) from point $(x_{\epsilon B}, y_1)$ to point $(x_{\gamma B}, y_1)$ gives

$$V_1 = \frac{kT(b_B-1)}{q(b_B+1)}\ln\left[\frac{n(x_{\epsilon B}, y_1)(b_B+1)+(p_{0B}-n_{0B})}{n(x_{\gamma B}, y_1)(b_B+1)+(p_{0B}-n_{0B})}\right] - \frac{kT}{q}\ln\left[\frac{n(x_{\epsilon B}, y_1)+(p_{0B}-n_{0B})}{n(x_{\gamma B}, y_1)+(p_{0B}-n_{0B})}\right]. \quad (21)$$

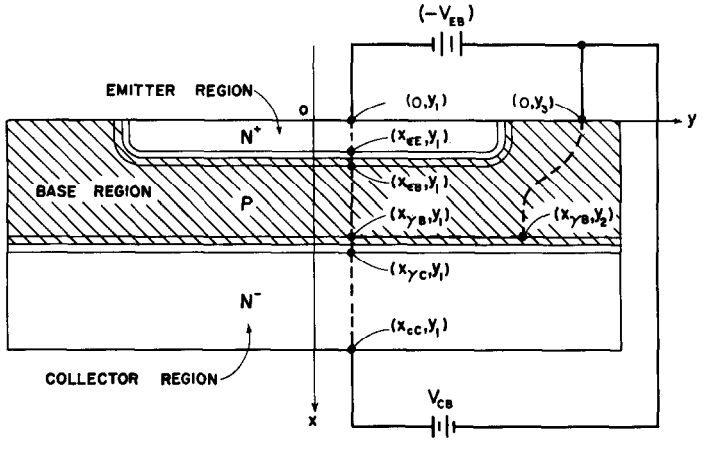

Fig. 4. Some two-dimensional features of the n^+pn^- transistor. The dotted lines represent paths of integration. This figure is similar to a corresponding figure given by van Vliet and Min[8].

Along the second part of the path the y component of $\vec{J}(x, y)$ is approximately zero and the integration of the second term in eqn (18) from point $(x_{\gamma B}, y_1)$ to point $(x_{\gamma B}, y_2)$ is equal to zero. The remaining integration is denoted by $+I_B R_{0B}$ which is the ohmic drop of the inactive base region of the transistor. Thus, the series potential drop from point $(x_{\epsilon B}, y_1)$ to point $(0, y_3)$ is given by

$$\psi(x_{\epsilon B}, y_1) - \psi(0, y_3) = -\frac{kT}{q} \ln \left[\frac{n(x_{\epsilon B}, y_1) + (p_{0B} - n_{0B})}{n(x_{\gamma B}, y_1) + (p_{0B} - n_{0B})} \right] - \frac{kT}{q} \left(\frac{b_B - 1}{b_B + 1} \right) \ln \left[\frac{n(x_{\gamma B}, y_1)(b_B + 1) + (p_{0B} - n_{0B})}{p_{0B} + b_B n_{0B}} \right] + I_B R_{0B}. \quad (22)$$

Substitution of this potential drop into eqn (17) gives

$$V_{EB} = V_{jE} - \frac{kT}{q} \ln \left(1 + \frac{n(x_{\epsilon B})}{N_{AB}} \right) + \frac{kT}{q} \ln \left(1 + \frac{n(x_{\gamma B})}{N_{AB}} \right) - \frac{kT}{q} \left(\frac{b_B - 1}{b_B + 1} \right) \ln \left[1 + (b_B + 1) \frac{n(x_{\gamma B})}{N_{AB}} \right] + I_B R_{0B} \quad (23)$$

where the previous one-dimensional notation is again used and the approximations from groups A and B of Table 2 have been employed. For simplicity, eqn (7) of the n^+pn^- transistor model is derived from eqn (23) by deletion of the last three terms from the latter equation.

To eliminate the need for two-dimensional notation in all subsequent equations, we will now make a brief initial examination of an expression for the collector-base voltage. From Fig. 4, this voltage is given by

$$V_{CB} = V_{jC} + [\psi(x_{cC}, y_1) - \psi(x_{\gamma C}, y_1)] + [\psi(x_{\gamma B}, y_1) - \psi(0, y_3)] \quad (24)$$

where the last term is equal to the last two terms of eqn (22). In one-dimensional notation, eqn (24) becomes

$$V_{CB} = V_{jC} + [\psi(x_{cC}) - \psi(x_{\gamma C})] - \frac{kT}{q} \left(\frac{b_B - 1}{b_B + 1} \right) \ln \left[1 + (b_B + 1) \frac{n(x_{\gamma B})}{N_{AB}} \right] + I_B R_{0B} \quad (25)$$

since $p_{0B} + b_B n_{0B}$ and $p_{0B} - n_{0B}$ are both approximately equal to N_{AB}.

The last two equations of the model are derived by an analysis which involves only the quasi-neutral collector region. Some of the assumptions required for this analysis have already been stated or implied, but are repeated here for emphasis:

(1) The five conventional semiconductor equations are applicable. These equations are the hole and electron continuity equations, the hole and electron transport equations, and the Poisson's equation.

(2) The electrical-neutrality equation can be used. A complete discussion of this approximation is given in Section 6.

(3) The collector region is doped uniformly and all impurity atoms are completely ionized. Recombination is negligible.

(4) Both the hole and electron mobilities are independent of local electric field and independent of location in the quasi-neutral collector region. Each mobility is a constant that is related to the corresponding diffusion coefficient by an Einstein relation.

(5) The flow lines for holes and electrons are parallel and uniformly spaced so that the various currents can be found from one-dimensional equations. The hole and electron current densities are independent of position.

(6) The quasi-neutral collector region is bounded by the collector-base space-charge region at one end and by the collector ohmic contact region at the other end. These two boundaries are plane surfaces which are perpendicular to the flow lines. The location of each boundary is fixed. The carrier concentrations at the collector ohmic boundary are given by their respective equilibrium values. That is, the ohmic contact can be described as a plane of infinite surface recombination velocity.

The derivation of eqns (8) and (9) proceeds as follows: The hole and electron transport equations are

$$J_n(x) = qD_{nC} \frac{dn}{dx} + q\mu_{nC} n(x) E(x) \quad (26)$$

and

$$J_p(x) = -qD_{pC} \frac{dp}{dx} + q\mu_{pC} p(x) E(x) \quad (27)$$

where general forms are used initially (e.g. the function $J_n(x)$ rather than the constant J_{nC}). The foregoing assumptions will be introduced only as required. Since $n(x) - p(x) = (n_{0C} - p_{0C})$ and $dn/dx = dp/dx$, eqns (26) and (27) become

$$J_n(x) = qD_{nC} \frac{dp}{dx} + q \left(\frac{q}{kT} D_{nC} \right) [p(x) + (n_{0C} - p_{0C})] E(x) \quad (28)$$

and

$$J_p(x) = -qD_{pC} \frac{dp}{dx} + q \left(\frac{q}{kT} D_{pC} \right) p(x) E(x) \quad (29)$$

if μ_{nC} and μ_{pC} are replaced by $(q/kT)D_{nC}$ and $(q/kT)D_{pC}$, respectively. Equation (29) can be solved for the electric field $E(x)$ to give

$$E(x) = \frac{kT}{q} \left[\frac{1}{p(x)} \frac{dp}{dx} + \frac{\gamma(x) J(x)}{qD_{pC} p(x)} \right] \quad (30)$$

where $\gamma(x)$ is defined as $J_p(x)/J(x)$. Substitution of eqn (30) into eqn (28) results in

$$J_n(x) = 2qb_C D_{pC} \left[1 + \frac{(n_{0C} - p_{0C})}{2p(x)} \right] \frac{dp}{dx} + b_C \left[1 + \frac{(n_{0C} - p_{0C})}{p(x)} \right] \gamma(x) J(x) \quad (31)$$

where b_C equals D_{nC}/D_{pC}. Because $J_n(x) = [1-\gamma(x)]J(x)$, eqn (31) is equivalent to

$$J(x) = qb_C D_{pC} \left\{ \frac{2p(x) + (n_{0C} - p_{0C})}{p(x)[1-\gamma(x)(b_C+1)] - \gamma(x) b_C (n_{0C} - p_{0C})} \right\} \frac{dp}{dx}. \quad (32)$$

Equation (8) of the n^+pn^- transistor model results directly from integrating eqn (32) through the quasi-neutral collector region—from the collector-base space-charge boundary at $x = x_{\gamma C}$ to the ohmic collector contact at $x = x_{cC}$. Note too that $D_{nC} = b_C D_{pC}$ and that, for the above assumptions, $\gamma_C = \gamma(x)$, $J(x) = -I_C/A_E$, $(n_{0C} - p_{0C}) = N_{DC}$, and $p(x_{cC}) = n_i^2/N_{DC}$. Substitution of eqn (32) in eqn (30) gives

$$E(x) = \frac{kT}{q} \left\{ \frac{[1+\gamma(x)(b_C-1)]}{p(x)[1-\gamma(x)(b_C+1)] - \gamma(x) b_C (n_{0C} - p_{0C})} \right\} \frac{dp}{dx} \quad (33)$$

The second term of eqn (25) is obtained by integrating eqn (33) through the quasi-neutral collector region. By dropping the third and fourth terms of eqn (25), we obtain eqn (9) of the model.

An implicit expression for the function $p(x)$ in the quasi-neutral collector region can be found by substituting a dummy variable z for $p(x)$ in eqn (32) and integrating the resulting equation from $z = p(x_{\gamma C})$ to $z = p(x)$. The result is

$$(x - x_{\gamma C})(I_C/A_E) = \frac{2qD_{nC}}{[1-\gamma_C(b_C+1)]} [p(x_{\gamma C}) - p(x)] + \frac{qD_{nC}(n_{0C} - p_{0C})[1+\gamma_C(b_C-1)]}{[1-\gamma_C(b_C+1)]} \ln \left\{ \frac{p(x_{\gamma C})[1-\gamma_C(b_C+1)] - \gamma_C b_C (n_{0C} - p_{0C})}{p(x)[1-\gamma_C(b_C+1)] - \gamma_C b_C (n_{0C} - p_{0C})} \right\}. \quad (34)$$

The behavior of the variable γ_C is an important feature of the n^+pn^- transistor model. If the n^+pn^- transistor is initially operating in the forward-active regime, this variable behaves as follows when the collector-base voltage V_{CB} is decreased and when the emitter-base voltage V_{EB} has a constant value: In the forward-active regime, γ_C decreases very slowly; it has a value which is always very slightly less than $(1/b_C)(n_i/N_{DC})^2$. In the quasi-saturation regime, γ_C decreases somewhat more rapidly until $\gamma_C = 0$ when $V_{CB} = 0$. In the forward-saturation regime, γ_C changes much more rapidly until γ_C approaches negative infinity at $I_C = 0$. In the reverse regime, γ_C decreases rapidly from positive infinity until its value is in the range from $(1/b_C)(n_i/N_{DC})^2$ to about unity. For values of γ_C in this range (and only in this range), the collector-base diode behaves like a forward-biased p^+n diode. Note that for the forward-active and quasi-saturation regimes, γ_C is always positive, which implies that holes are *emitted from* the collector region through the base region into the emitter region. For the forward-saturation and the reverse regimes, the n^+pn^- transistor model predicts that holes are injected from the base region into the collector region. The infinite value of γ_C when $I_C = 0$ has a clear physical interpretation. If electrons are injected from the emitter region through the base region into the collector region, then a zero value of the collector current can result only if equal numbers of holes are also injected from the base region into the collector region. For such a condition, $I_p(x)$ cancels $I_n(x)$ at every point in the collector region and it follows that γ_C has an infinite value.

3. AN ABRIDGED n^+pn^- TRANSISTOR MODEL

In general, eqns (1) through (9) making up the n^+pn^- transistor model are difficult to use for numerical calculations. However, these equations can be abridged for the forward-active and quasi-saturation regimes. The resulting equations are:

$$I_B = K_B \left[\exp \frac{q(-V_{EB})}{kT} \right] \quad (35)$$

$$n(x_{\epsilon B}) = -\frac{N_{AB}}{2} + \sqrt{\left(\left(\frac{N_{AB}}{2} \right)^2 + n_i^2 \left[\exp \frac{q(-V_{EB})}{kT} \right] \right)} \quad (36)$$

$$V_{jC} = -\frac{kT}{q} \ln \left\{ \frac{N_{DC} N_{AB}}{n_i^2} \times \left[\frac{-N_{AB} + \sqrt{(N_{AB}^2 + 4p(x_{\gamma C})[p(x_{\gamma C}) + N_{DC}])}}{2[p(x_{\gamma C}) + N_{DC}]} \right] \right\} \quad (37)$$

$$n(x_{\gamma B}) = \frac{n_i^2}{N_{AB}} \left(\exp \frac{q(-V_{jC})}{kT} \right) \left[\frac{1 + \left(\frac{n_i}{N_{DC}} \right)^2 \exp \frac{q(-V_{jC})}{kT}}{1 - \left[\frac{n_i}{N_{AB}} \frac{n_i}{N_{DC}} \exp \frac{q(-V_{jC})}{kT} \right]^2} \right] \quad (38)$$

$$I_C = qA_E \frac{D_{nB}}{X_B} \left\{ 2[n(x_{\epsilon B}) - n(x_{\gamma B})] - N_{AB} \ln \left[\frac{n(x_{\epsilon B}) + N_{AB}}{n(x_{\gamma B}) + N_{AB}} \right] \right\} \quad (39)$$

$$V_{CB} = V_{jC} + \frac{kT}{q} \left[\frac{X_C I_C}{qA_E D_{nC} N_{DC}} - 2\frac{p(x_{\gamma C})}{N_{DC}} \right] \quad (40)$$

$$V_{jE} = -\frac{kT}{q} \left[\ln \frac{N_{AB} n(x_{\epsilon B})}{n_i^2} \right] \quad (41)$$

$$p(x_{\epsilon E}) = \left(\frac{n_{iE}}{n_i} \right)^2 \frac{N_{AB}}{N_{DE}} n(x_{\epsilon B}) \left[1 + \frac{n(x_{\epsilon B})}{N_{AB}} \right] \quad (42)$$

$$\gamma_C = \frac{1}{b_C} \left(\frac{n_i}{N_{DC}} \right)^2 - \frac{p(x_{\gamma C})}{b_C N_{DC}} \left[\exp \frac{q(V_{jC} - V_{CB})}{kT} \right]. \quad (43)$$

By assuming values for V_{EB} and $p(x_{\gamma C})$, we can readily calculate the values of the remaining nine variables if the above nine equations are employed in the given sequence.

Equations (35) through (43) are derived as follows: Equations (1) and (5) yield

$$I_B = qA_E \frac{D_{pE}}{L_{pE}} \frac{n_{iE}^2}{N_{DE}} \left(\exp \frac{q(-V_{jE})}{kT}\right) \left[1 + \frac{n_i^2}{N_{AB}^2} \exp \frac{q(-V_{jE})}{kT}\right] \tag{44}$$

since $p(x_{\epsilon E}) \gg n_{iE}^2/N_{DE}$ and $I_B \gg \gamma_C I_C$. Equation (7) can be rewritten

$$(-V_{jE}) = (-V_{EB}) - \frac{kT}{q} \ln \left[1 + \frac{n_i^2}{N_{AB}^2} \exp \frac{q(-V_{jE})}{kT}\right]. \tag{45}$$

Substituting eqn (45) in the argument of the first exponential factor of eqn (44) leads to cancellation of the factors in square brackets, so that the base current I_B is given by eqn (35) where K_B is defined as $qA_E D_{pE} n_{iE}^2/(L_{pE} N_{DE})$. In other words, the emitter defect current (accounting for all of the base current in the n^+pn^- transistor) has simple exponential dependence on the *terminal* voltage V_{EB} for low, intermediate and high currents in the base region. Physically, this important result occurs because the Webster effect involves a growing *majority-carrier* concentration at the base boundary of the emitter-base space-charge region; accompanying this is a faster-than-Boltzmann increase in the *minority-carrier* concentration at the emitter boundary of the same region, and this effect turns out to be just sufficient to compensate for the fact that the emitter-base junction voltage V_{jE} is less than the applied emitter-base voltage V_{EB}.

Equations (2) and (7) combine to give an equation relating $n(x_{\epsilon B})$ and V_{EB}. The solution of this equation for $n(x_{\epsilon B})$ gives eqn (36). The solution of eqn (4) for V_{jC} yields eqn (37). Equation (3) is repeated as eqn (38). With $1 \gg |\gamma_C|$, eqn (6) becomes eqn (39). With $1 \gg \gamma_C(b_C + 1) > \gamma_C(b_C - 1) > \gamma_C$, eqns (8) and (9) combine to give eqn (40). The solution of eqn (2) for V_{jE} gives eqn (41). Substitution of this equation into eqn (1) results in eqn (42). With the approximation that $\gamma_C \ll 1$, eqn (9) can be solved for γ_C to give eqn (43).

Equations (35) through (43) yield the common-emitter characteristics shown in Fig. 5. Note that these characteristics are plotted using V_{CB} rather than V_{CE}. Theoretical characteristics are usually easier to plot if the collector-base voltage is employed; experimental characteristics, if the collector-emitter voltage is employed. For point A indicated on Fig. 5, the values of the eleven variables are given in Table 3. Also given in this table are the parameters used for Fig. 5.

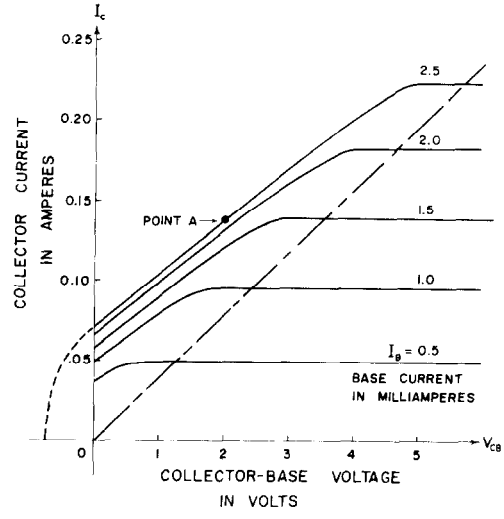

Fig. 5. The common-emitter characteristics of the n^+pn^- transistor when the collector-base voltage is employed as a variable. The solid curves represent the characteristics as predicted by the abridged model. The numerical data corresponding to point A are given in Table 3. The dotted curve represents an extension of one characteristic into the forward-saturation regime of operation where eqns (1)–(9) must be employed.

The hole- and electron-concentration profiles that correspond to point A of Fig. 5 are shown in Fig. 6(a). The corresponding electrostatic-potential profile is shown in Fig. 6(b) where the zero value of this potential is defined by the arbitrary condition that $\psi(x_{\epsilon B}) = -(kT/q) \exp[p(x_{\epsilon B})/n_i]$. Two auxiliary profiles for the hole and electron quasi-Fermi potentials (imrefs) are also shown in Fig. 6(b). The hole quasi-Fermi potential is equal to zero at the boundary between the active base region and the emitter-base space-charge region as a result of the arbitrarily set zero value for the electrostatic potential. If hole current is negligible in the base and collector regions of an n^+pn^- transistor operating in the quasi-saturation regime, then the hole quasi-Fermi potential is approximately constant and equal to zero in the active base region, in the two space-charge regions and in the conductivity modulated portion of the quasi-neutral collector region.

Table 3. Numerical values. This Table corresponds to point A of Fig. 5

$V_{EB} = -0.795$ V	$V_{CB} = 2.002$ V	$I_C = 0.1378$ A	$I_B = 0.0025$ A
$V_{jE} = -0.790$ V	$V_{jC} = -0.694$ V	$\gamma_C = (1.26 \cdot 10^{-11} - 3.68 \cdot 10^{-45})$	
$p(x_{\epsilon E}) = 2.87 \cdot 10^{13}/cm^3$	$n(x_{\epsilon B}) = 2.33 \cdot 10^{16}/cm^3$	$n(x_{\gamma B}) = 9.40 \cdot 10^{15}/cm^3$	$p(x_{\gamma C}) = 3.11 \cdot 10^{16}/cm^3$
$N_{DE} = 1.0 \cdot 10^{20}/cm^3$	$N_{AB} = 1.0 \cdot 10^{17}/cm^3$	$N_{DC} = 2.0 \cdot 10^{15}/cm^3$	$n_i = 1.15 \cdot 10^{10}/cm^3$
$K_B = 1.15 \cdot 10^{-16}$ A	$\mu_{nB} = 7.0 \cdot 10^2 cm/V\,sec$	$\mu_{nC} = 1.23 \cdot 10^3 cm/V\,sec$	$q = 1.6 \cdot 10^{-19}$ coul
$A_E = 1.5 \cdot 10^{-4} cm^2$	$X_B = 5.0 \cdot 10^{-5} cm$	$X_C = 1.5 \cdot 10^{-3} cm$	$kT/q = 0.0259$ V
$n_{iE} = 1.15 \cdot 10^{10}/cm^3$		$b_C = 2.617$	
$\beta_F = 55.1$	$h_{fe} = 13.8$	$f(V_{jC}) = 1.027$	$r_o/R_o = 1.21$
$\xi_1 = 1.10$	$\xi_1^* = 1.13$	$Q_{CO}/Q_{BO} = 0.600$	$R_o = 25.4\ \Omega$
$\xi_2 = 1.04$	$\xi_2^* = 1.06$	$Q_B^*/Q_{BO} = 0.165$	$g(Q_C^*) = 0.728$
$\xi_3 = 2.06$	$\xi_3^* = 1.88$	$Q_C^*/Q_{BO} = 1.141$	$Q_{BO} = 1.20 \cdot 10^{-10}$ coul

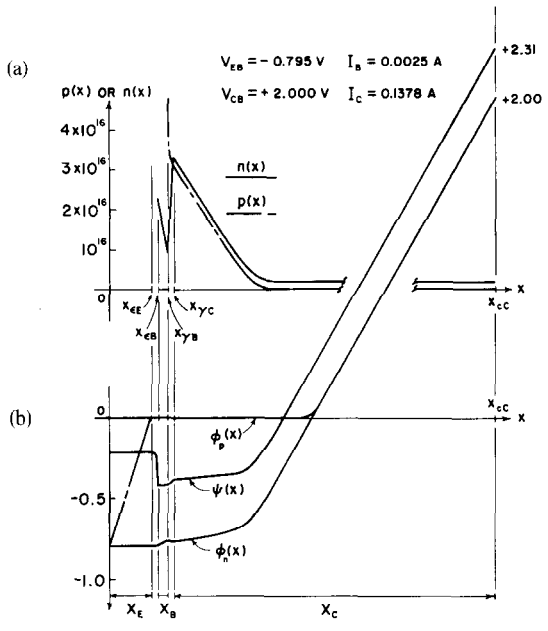

Fig. 6. The hole-concentration, electron-concentration and electrostatic-potential profiles. The operating conditions correspond to point A of Fig. 5.

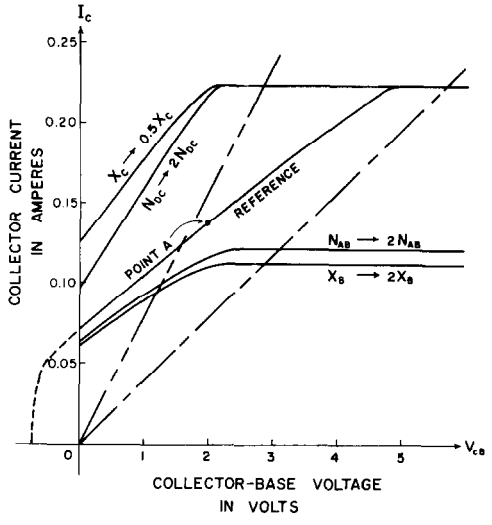

Fig. 7. The effects of variations in the structural parameters. The reference curve of this figure is identical to the curve given in Fig. 5 for $I_B = 2.5$ mA.

In Fig. 6(b), the small potential rise across the collector-base space-charge region is an important feature of the electrostatic-potential profile: It represents a barrier to the flow of holes from the active base region to the quasi-neutral collector region. If this barrier did not exist, then majority carriers would contribute substantially to the flow of current in the active base region. Furthermore, the collector-base junction voltage V_{jC} would be equal to or greater than the built-in voltage ψ_{oC} of this junction. Both these conditions are physically unrealistic.

The slope of the minority carrier concentration at the position $x_{\epsilon B}$ is always negative for positive values of collector current even if the whole collector region becomes highly conductivity modulated. Furthermore, if the hole current is negligible in the base and collector regions, then the current transport in the base region is by drift and diffusion of minority carriers (electrons) and the current transport in the collector region is by drift and diffusion of majority carriers (again electrons).

The collector-base characteristics of five n^+pn^- transistors are indicated in Fig. 7. The reference curve is identical to the n^+pn^- transistor curve given in Fig. 5 for $I_B = 2.5$ mA. Each of the remaining curves represents the corresponding characteristic of a modified transistor which is identical to the reference transistor except for one parameter. For the top curve, the notation $X_C \rightarrow (1/2)X_C$ indicates that the thickness of the collector region of the modified transistor associated with this curve is one half the thickness of the collector region of the reference transistor. For the three remaining curves, the corresponding modifications involve the collector doping concentration N_{DC}, the base doping concentration N_{AB}, and the base thickness X_B. Note that the top two curves represent two transistors with the same collector resistance and the bottom two curves represent another two transistors with the same Gummel number [22].

4. LOW-FREQUENCY SMALL-SIGNAL CHARACTERISTICS

If $V_{CB} > 0$, the small-signal current gain h_{fe} and the small-signal output resistance r_o can be calculated directly from the abridged n^+pn^- transistor model that consists of eqns (35) through (43). The calculation proceeds as follows: The variation of eqn (35) gives

$$\delta I_B = I_B \frac{q}{kT}(-\delta V_{EB}) \tag{46}$$

where δ denotes a small, finite change in the following variable. The variation of eqn (36) results in

$$\delta n(x_{\epsilon B}) = \left[\frac{n(x_{\epsilon B}) + N_{AB}}{2n(x_{\epsilon B}) + N_{AB}}\right] n(x_{\epsilon B}) \frac{q}{kT}(-\delta V_{EB}). \tag{47}$$

The variation of eqn (38) gives an expression relating δV_{jC} and $\delta n(x_{\gamma B})$. The variation of eqn (37) gives an expression relating $\delta p(x_{\gamma C})$ and δV_{jC}. The elimination of δV_{jC} from these two expressions results in

$$\delta n(x_{\gamma B}) = \left[\frac{2p(x_{\gamma C}) + N_{DC}}{2n(x_{\gamma B}) + N_{AB}}\right] \delta p(x_{\gamma C}). \tag{48}$$

The variation of eqn (39) gives

$$\delta I_C = qA_E \frac{D_{nB}}{X_B}\left\{\left[\frac{2n(x_{\epsilon B}) + N_{AB}}{n(x_{\epsilon B}) + N_{AB}}\right] \delta n(x_{\epsilon B}) - \left[\frac{2n(x_{\gamma B}) + N_{AB}}{n(x_{\gamma B}) + N_{AB}}\right] \delta n(x_{\gamma B})\right\}. \tag{49}$$

Equation (46) can be solved for δV_{EB} and the solution can be substituted into eqn (47). The resulting expression

and eqn (48) can be substituted into eqn (49) to give

$$\delta I_C = qA_E \frac{D_{nB}}{X_B} \left\{ n(x_{eB}) \frac{\delta I_B}{I_B} - \left[\frac{2p(x_{\gamma C}) + N_{DC}}{n(x_{\gamma B}) + N_{AB}} \right] \delta p(x_{\gamma C}) \right\}. \quad (50)$$

The variation of eqn (37) and the variation of eqn (40) can be combined to give

$$\delta p(x_{\gamma C}) = \frac{N_{DC}}{2} \left[\frac{X_C \delta I_C}{qA_E D_{nC} N_{DC}} - \frac{q}{kT} (\delta V_{CB}) \right] \frac{1}{f(V_{jC})} \quad (51)$$

where the function $f(V_{jC})$ will be subsequently defined. The insertion of eqn (51) into eqn (50) results in

$$\left[1 + \frac{1}{2} \left(\frac{2p(x_{\gamma C}) + N_{DC}}{n(x_{\gamma B}) + N_{AB}} \right) \frac{D_{nB}}{D_{nC}} \frac{X_C}{X_B} \frac{1}{f(V_{jC})} \right] \delta I_C = \left[qA_E \frac{D_{nB}}{X_B} n(x_{eB}) \frac{1}{I_B} \right] \delta I_B + \left[\frac{qA_E \mu_{nC} N_{DC}}{X_C} \frac{1}{2} \times \left(\frac{2p(x_{\gamma C}) + N_{DC}}{n(x_{\gamma B}) + N_{AB}} \right) \frac{D_{nB}}{D_{nC}} \frac{X_C}{X_B} \frac{1}{f(V_{jC})} \right] \delta V_{CB}. \quad (52)$$

By defininition, the small-signal current gain and the small-signal output resistance are given by $h_{fe} = \partial I_C / \partial I_B$ and $r_0 = \partial V_{CB} / \partial I_C$, respectively. Thus, it follows from eqn (52) that

$$h_{fe} = \frac{qA_E (D_{nB}/X_B) n(x_{eB})}{I_B (1 + B)} \quad (53)$$

and

$$r_0 = \frac{X_C}{q\mu_{nC} N_{DC} A_E} \left[1 + \frac{1}{B} \right] \quad (54)$$

where the variable B is defined as

$$B = \frac{1}{2} \left[\frac{1 + 2 \dfrac{p(x_{\gamma C})}{N_{DC}}}{1 + \dfrac{n(x_{\gamma B})}{N_{AB}}} \right] \left(\frac{N_{DC} X_C / D_{nC}}{N_{AB} X_B / D_{nB}} \right) \frac{1}{f(V_{jC})}. \quad (55)$$

The first factor in eqn (54) represents the equilibrium ohmic resistance of the collector region and the second factor embodies the modification produced by high currents. For point A shown in Fig. 5, the second factor is approximately 1.2. Thus, the slope at point A of Fig. 5 corresponding to $I_B = 2.5$ mA is approximately equal to the conductivity of the collector region at equilibrium. Equation (53) was used to plot the small-signal current gain h_{fe} as a function of I_C and the result is shown in Fig. 8. Also given is the large-signal current gain β_F which was calculated from eqn (35) through (40). The falloff of h_{fe} as I_C increases is much more rapid than is the falloff of β_F. Note that h_{fe} can be less than one-half of β_F in the "fall off" region.

The function $f(V_{jC})$ can usually be approximated by unity so that the evaluation of eqn (55) is straightforward. This function is

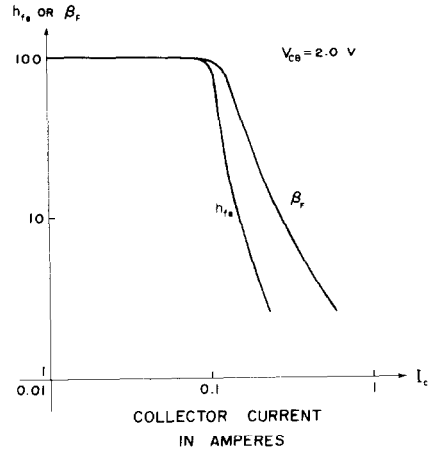

Fig. 8. The a.c. and d.c. current gains. Note that the falloff of the a.c. current gain is more rapid than the falloff of the d.c. current gain, as the collector current is increased.

$$f(V_{jC}) = 1 + \left\{ \frac{1}{2} \frac{[1 - x^2]^2 / x}{[(N_{AB}/N_{DC})(1 + x^2) + 2x]} \right\} \quad (56)$$

where

$$x = \frac{n_i^2}{N_{AB} N_{DC}} \exp \frac{q(-V_{jC})}{kT}. \quad (57)$$

5. A CHARGE-CONTROL RELATION

The first five equations of the abridged model can be used to derive a charge-control relation as follows: The link between $n(x_{\gamma B})$ and $p(x_{\gamma C})$ as given by eqns (37) and (38) is equivalently given by

$$n(x_{\gamma B}) = \frac{p(x_{\gamma C})^2}{N_{AB}} \left(\frac{2}{\xi_3} \right) \quad (58)$$

where ξ_3 is a function of $n(x_{\gamma B})$ and $p(x_{\gamma C})$ and is a slowly varying function in the quasi-saturation regime. Note that eqn (58) defines the variable ξ_3. This and other such variables are introduced in this section so that the resulting charge-control relation has relatively simple form. Equation (36) can be rewritten as

$$n(x_{eB}) = \frac{n_i^2}{N_{AB}} \left(\exp \frac{q(-V_{EB})}{kT} \right) \left\{ \frac{1}{1 + [n(x_{eB})/N_{AB}]} \right\}. \quad (59)$$

Equation (39) is equivalent to

$$I_C = qA_E \frac{D_{nB}}{X_B} [\xi_1 n(x_{eB}) - \xi_2 n(x_{\gamma B})] \quad (60)$$

Where ξ_1 and ξ_2 are bounded functions whose values are in the range from unity to two. Substitution of eqns (58) and (59) into eqn (60) gives

$$I_C = qA_E \frac{\xi_1 D_{nB}}{X_B}\left(\frac{n_i^2}{N_{AB}}\right)\left\{\frac{\exp[q(-V_{EB})/(kT)]}{1+[n(x_{\epsilon B})/N_{AB}]} - \frac{\xi_2}{\xi_1}\frac{2}{\xi_3}\left(\frac{p(x_{\gamma C})}{n_i}\right)^2\right\}. \quad (61)$$

This equation can be written as

$$I_C = \frac{(qA_E n_i)^2 \xi_1 D_{nB}}{Q_{B0}} \frac{\left[\exp\frac{q(-V_{EB})}{kT}\right]}{\left[1+\frac{n(x_{\epsilon B})}{N_{AB}}\right]\left[1+\xi_2\frac{2}{\xi_3}\frac{qA_E D_{nB} p(x_{\gamma C})^2}{X_B N_{AB} I_C}\right]} \quad (62)$$

in which Q_{B0} is defined as $qA_E X_B N_{AB}$. To put eqn (62) in a charge-control form, we must introduce two charge-control variables which are defined as follows:

$$Q_B^* = qA_E \int_{x_{\epsilon B}}^{x_{\gamma B}} n(x)\,dx \quad (63)$$

$$Q_C^* = qA_E \int_{x_{\gamma C}}^{x_{cC}} p(x)\,dx. \quad (64)$$

Equation (63) can be integrated by changing the variable of integration from x to $n(x)$ and by employing then eqn (20) in a one-dimensional form. The result of the integration is

$$Q_B^* = \frac{(qA_E)^2 D_{nB}}{I_C}\left\{[n(x_{\epsilon B})^2 - n(x_{\gamma B})^2] - [n(x_{\epsilon B}) - n(x_{\gamma B})](p_{0B} - n_{0B}) + (p_{0B} - n_{0B})^2 \ln\left[\frac{n(x_{\epsilon B}) + (p_{0B} - n_{0B})}{n(x_{\gamma B}) + (p_{0B} - n_{0B})}\right]\right\}. \quad (65)$$

Similarly, eqn (64) can be integrated by changing the variable of integration from x to $p(x)$ and by employing then eqn (32). The result of this integration is

$$Q_C^* = \frac{(qA_E)^2 D_{nC}}{I_C}\left\{[p(x_{\gamma C})^2 - p_{0C}^2] + \left[\frac{1+\gamma_C(b_C-1)}{1-\gamma_C(b_C+1)}\right][p(x_{\gamma C}) - p_{0C}](n_{0C} - p_{0C}) + (n_{0C} - p_{0C})^2 \frac{[1+\gamma_C(b_C-1)]}{[1-\gamma_C(b_C+1)]^2}\gamma_C b_C \ln\left[\frac{p(x_{\gamma C})[1-\gamma_C(b_C+1)] - \gamma_C b_C(n_{0C} - p_{0C})}{p_{0C}[1-\gamma_C(b_C+1)] - \gamma_C b_C(n_{0C} - p_{0C})}\right]\right\}. \quad (66)$$

With the approximations of groups A and B of Table 2, eqns (65) and (66) can be rewritten as

$$Q_B^* = \frac{(qA_E)^2 D_{nB}}{I_C}\left[\left(\frac{\xi_1^*}{2}\right)n(x_{\epsilon B})^2 - \left(\frac{\xi_2^*}{2}\right)n(x_{\gamma B})^2\right] \quad (67)$$

$$Q_C^* = (qA_E)^2 D_{nC}\frac{p(x_{\gamma C})^2}{I_C}\left(\frac{2}{\xi_3^*}\right) \quad (68)$$

where ξ_1^*, ξ_2^* and ξ_3^* are functions of $n(x_{\epsilon B})$, $n(x_{\gamma B})$ and $p(x_{\gamma C})$, respectively. Equation (68) can be solved for $p(x_{\gamma C})$ and then the resulting equation can be substituted into eqn (62) to give

$$I_C = \frac{(qA_E n_i)^2 \xi_1 D_{nB}}{Q_{B0}} \frac{\left[\exp\frac{q(-V_{EB})}{kT}\right]}{\left[1+\frac{n(x_{\gamma B})}{N_{AB}}\right]\left[1+\xi_2\frac{\xi_3^*}{\xi_3}\frac{D_{nB}}{D_{nC}}\frac{Q_C^*}{Q_{B0}}\right]}. \quad (69)$$

Equations (58), (60), (67) and (68) can be combined to give

$$Q_B^* = \frac{Q_{B0}}{2N_{AB}}\left[\frac{\xi_1^* n(x_{\epsilon B})^2 - \xi_2^* n(x_{\gamma B})^2}{\xi_1 n(x_{\epsilon B}) - \xi_2 n(x_{\gamma B})}\right] \quad (70)$$

$$Q_C^* = Q_{B0}\frac{D_{nC}}{D_{nB}}\left[\frac{n(x_{\gamma B})}{\xi_1 n(x_{\epsilon B}) - \xi_2 n(x_{\gamma B})}\right]\frac{\xi_3}{\xi_3^*}. \quad (71)$$

Equations (70) and (71) can be simultaneously solved for $n(x_{\epsilon B})$.Dividing the resulting expression by N_{AB} gives

$$\frac{n(x_{\epsilon B})}{N_{AB}} = \frac{Q_B^*}{Q_{B0}}\left(\frac{\xi_1}{\xi_1^*}2g(Q_C^*)\right) \quad (72)$$

where the function $g(Q_C^*)$ is given by

$$q(Q_C^*) = \left\{\frac{\left[1+\frac{Q_C^*}{Q_{B0}}\left(\xi_2\frac{\xi_3^*}{\xi_3}\frac{D_{nB}}{D_{nC}}\right)\right]}{\left[1+\frac{Q_C^*}{Q_{B0}}\left(\xi_2\frac{\xi_3^*}{\xi_3}\frac{D_{nB}}{D_{nC}}\right)\right]^2 - \frac{\xi_2^*}{\xi_1^*}\left[\frac{Q_C^*}{Q_{B0}}\left(\xi_1\frac{\xi_3^*}{\xi_3}\frac{D_{nB}}{D_{nC}}\right)\right]^2}\right\} \quad (73)$$

The function $g(Q_C^*)$ has values in the range from zero to unity. Substitution of eqn (72) into eqn (69) gives

$$I_C = \frac{(qA_E n_i)^2 \xi_1 D_{nB}\exp\left[\frac{q(-V_{EB})}{kT}\right]}{Q_{B0}\left[1+\frac{Q_B^*}{Q_{B0}}\left(\frac{\xi_1}{\xi_1^*}2g(Q_C^*)\right)\right]\left[1+\frac{Q_C^*}{Q_{B0}}\left(\xi_2\frac{\xi_3^*}{\xi_3}\frac{D_{nB}}{D_{nC}}\right)\right]} \quad (74)$$

which is the desired charge control relation. Note that we have not introduced new approximations in this section. That is, eqn (74) is exactly equivalent to the first six equations of the abridged model. Moreover, eqn (74) is nearly consistent with the following extended form of Gummel's relation[23]:

$$I_C = \frac{(qA_E n_i)^2 D_{nB}\left[\exp\frac{q(-V_{EB})}{kT}\right]}{(Q_{B0} + Q_B^* + Q_C^*)}. \quad (75)$$

For point A values, this equation yields a value for I_C which is about 23% less than given by eqn (74). Further details relating to the last two equations are given in Section 7 below.

6. ELECTRICAL NEUTRALITY

Ambipolar diffusion is inevitably accompanied by an "internal" field[24]. That is, there exists a finite space charge in the quasi-neutral volume under consideration, and consequently a spatially varying electric field. This "source charge" density, as it has been aptly termed, is provided by the diffusing species themselves by a slight imbalance of their populations relative to one another. There are a large number of problems of practical interest, and fortunately the present one is among them, where the magnitude of the source-charge density is negligible relative to certain densities describing the distributions of the diffusing species. In the present problem, the relevant descriptive charge densities are the excess hole charge density $q[p(x)-p_0]$ and the excess electron charge density $q[n(x)-n_0]$. For ambipolar diffusion the source-charge density, which is given by $q[p(x)-n(x)-(p_0-n_0)]$, must be negligible relative to both $q[p(x)-p_0]$ and $q[n(x)-n_0]$.

The significance of having $q[p(x)-n(x)-(p_0-n_0)]$ much less than both $q[p(x)-p_0]$ and $q[n(x)-n_0]$ is that as a result, $p(x)-p_0=n(x)-n_0$ remains a good approximation and consequently also, $dp/dx = dn/dx$ provided that p_0 and n_0 are constants. Therefore, it is standard practice to set $[p(x)-n(x)-(p_0-n_0)]$ equal to zero. This condition which is known as electrical neutrality has been a cause of considerable confusion in the literature. Frequently, the electrical-neutrality condition will be substituted into Poisson's equation to give the illogical result that the electric field is a constant in a quasi-neutral semiconductor region. The confusion can perhaps be removed by the following discussion.

For the collector region of the n^+pn^- transistor, the standard semiconductor equations reduce to

$$\gamma_C J = -qD_{pC}\frac{dp}{dx} + q\mu_{pC}p(x)E(x) \tag{76}$$

$$(1-\gamma_C)J = qD_{nC}\frac{dn}{dx} + q\mu_{nC}n(x)E(x) \tag{77}$$

and

$$\frac{dE}{dx} = \frac{q}{\epsilon}[p(x)-n(x)-(p_{0C}-n_{0C})] \tag{78}$$

where J is the total current and γ_C is the ratio of $J_p(x)$ to J. A direct solution of these equations is rarely possible. Consequently, for the reasons justified qualitatively above, the problem given by eqns (76) through (78) is replaced by a related problem which involves the following three equations

$$\gamma_C J = -qD_{pC}\frac{dp_A}{dx} + q\mu_{pC}p_A(x)E_A(x) \tag{79}$$

$$(1-\gamma_C)J = qD_{nC}\frac{dn_A}{dx} + q\mu_{nC}n_A(x)E_A(x) \tag{80}$$

$$p_A(x)-n_A(x)-(p_{0C}-n_{0C}) = 0. \tag{81}$$

In these equations, the subscript A which stands for "approximate" indicates that, for example, the function $p(x)$ is not identical to $p_A(x)$. The functions $p_A(x)$, $n_A(x)$ and $E_A(x)$ as determined by eqns (79)–(81) approximate the corresponding functions $p(x)$, $n(x)$ and $E(x)$ as determined by eqn (76)–(78) provided that

$$+\epsilon(dE_A/dx) \ll q[p_A(x)-p_{0C}] \tag{82}$$

and

$$+\epsilon(dE_A/dx) \ll q[n_A(x)-n_{0C}]. \tag{83}$$

If an approximate source-charge density is defined as

$$\rho_A(x) \equiv \epsilon(dE_A/dx) \tag{84}$$

then eqns (82) and (83) state that $\rho_A(x)$ is much less than both the approximate excess charge densities $q[p_A(x)-p_0]$ and $q[n_A(x)-n_0]$.

Our aim in this section is to calculate $\rho_A(x)$ for the collector region of an n^+pn^- transistor and to employ this variable to determine a condition for the validity of eqns (8) and (9). For the calculation of $\rho_A(x)$, eqns (32) and (33) are rewritten here with the subscript A added to each variable:

$$J = qb_C D_{pC}\left\{\frac{2p_A(x)+(n_{0C}-p_{0C})}{p_A(x)[1-\gamma_C(b_C+1)]-\gamma_C b_C(n_{0C}-p_{0C})}\right\}\frac{dp_A}{dx} \tag{85}$$

$$E_A(x) = \frac{kT}{q}\left\{\frac{1+\gamma_C(b_C-1)}{p_A(x)[1-\gamma_C(b_C+1)]-\gamma_C b_C(n_{0C}-p_{0C})}\right\}\frac{dp_A}{dx}. \tag{86}$$

Equation (85) can be solved for dp_A/dx and the solution can be substituted in eqn (86) to give

$$E_A(x) = \frac{kT}{q}\frac{J}{qD_{nC}}\left[\frac{1+\gamma_C(b_C-1)}{2p_A(x)+(n_{0C}-p_{0C})}\right] \tag{87}$$

since $b_C D_{pC} = D_{nC}$. Substitution of eqn (87) into eqn (84) yields

$$\rho_A(x) = \frac{kT}{q}\frac{\epsilon J 2}{qD_{nC}}\frac{[1+\gamma_C(b_C-1)]}{[2p_A(x)+(n_{0C}-p_{0C})]^2}\frac{dp_A}{dx} \tag{88}$$

Equations (85) and (88) can be combined to give

$$\rho_A(x) = 4q\left(\frac{\epsilon kT}{2q^2N_{DC}}\right)\left(\frac{I_C}{qA_E D_{nC}N_{DC}}\right)^2 \left\{\frac{p_A(x)[1-\gamma_C(b_C+1)]-\gamma_C b_C N_{DC}}{\left[1+2\frac{p_A(x)}{N_{DC}}\right]^3}\right\}[1+\gamma_C(b_C-1)] \tag{89}$$

since $J = -I_C/A_E$ and $n_{0C}-p_{0C} = N_{DC}$. If I_3 is defined

as the value of I_C for which the maximum value of $[\rho_A(x)/q]$ divided by $[p_A(x) - p_{0C}]$ is equal to unity, then it follows that I_3 is approximately given by

$$I_3 = \frac{1}{2}\frac{qA_E D_{nC} N_{DC}}{\sqrt{(\epsilon kT/(2q^2 N_{DC}))}} \tag{90}$$

provided that $p_A(x_{\gamma C}) \gg n_i$. Note that I_3 is proportional to $N_{DC}^{3/2}$ and independent of X_C. One condition for validity of eqns (8) and (9) is that $I_C < I_3$. Our numerical calculations indicate that eqns (8) and (9) may be quite satisfactory for values of I_C slightly greater than I_3. For the numerical calculations given in this paper, we have assumed that eqns (8) and (9) are valid if $I_C < 2I_3$.

It appears that the n^+pn^- transistor model can be extended for $I_C > I_3$ if an additional space-charge region is introduced in the collector region.

7. DISCUSSION OF THE n^+pn^- TRANSISTOR MODEL

As has been noted, eqns (1) through (9) predict the approximate characteristics of n^+pn^- transistor operating with $I_C < I_3$. The n^+pn^- transistor model which consists of these nine equations is most accurate for the quasi-saturation regime. It is somewhat less accurate for the forward-active and forward-saturation regimes. It is probably accurate for the reverse regime.

For the forward-active regime, the model fails to predict the Early effect[25] because $x_{\gamma B}$ and $x_{\gamma C}$ are assumed to be fixed. The model could be extended by making $x_{\epsilon B}$ and $x_{\gamma B}$ functions of V_{jC} or by introducing an Early voltage[2]. It is interesting to note that the model does predict a pseudo Early voltage when $x_{\epsilon B}$ and $x_{\gamma B}$ are fixed. This voltage results from the modulation of $n(x_{\gamma B})$ as V_{CB} is changed. The conventional Early voltage and the Early effect itself are associated primarily with the modulation of $x_{\gamma B}$ as V_{CB} is changed. The pseudo Early voltage is very large (>100 V) and effects associated with this voltage are normally negligible.

For the forward-saturation regime, the model is somewhat inaccurate because of certain approximations that are associated with the two-dimensional effects in the base region. A more accurate model is perhaps unnecessary since the parasitic resistances of any real transistor will largely determine the actual characteristics for this regime.

For the reverse regime, the model appears to be accurate. Preliminary calculations have been completed indicating that eqns (6) and (7) will require only slight modifications for this regime.

The essential features of the n^+pn^- transistor model are given by the following four equations:

$$n(x_{\gamma B}) = \frac{p(x_{\gamma C})^2}{N_{AB}} \tag{91}$$

$$n(x_{\epsilon B}) = \frac{n_i^2}{N_{AB}} \exp\left[\frac{q(-V_{EB})}{kT}\right] \tag{92}$$

$$I_C = qA_E \frac{D_{nB}}{X_B}[n(x_{\epsilon B}) - n(x_{\gamma B})] \tag{93}$$

$$p(x_{\gamma C})^2 = (qA_E)^2 D_{nC} Q_C^* I_C. \tag{94}$$

Equation (91) is an approximate form of eqn (58); eqn (92), of eqn (59); eqn (93), of eqn (60); and eqn (94), of eqn (68). The last three equations written above have been frequently used for analytical models of bipolar transistors. The first equation provides the critical link between base-region phenomena and collector-region phenomena.

The above four approximate equations can be combined into a single equation that resembles Gummel's relation. Equation (94) is substituted into eqn (91). The resulting equation and eqn (92) are substituted into eqn (93) to give an expression relating I_C, V_{EB} and Q_C^*. Solving this expression for I_C yields

$$I_C = \frac{(qA_E n_i)^2 D_{nB} \exp\dfrac{q(-V_{EB})}{kT}}{Q_{B0} + Q_C^*} \tag{95}$$

where Q_{B0} is $qA_E N_{AB} X_B$, as before. This approximate equation predicts characteristics which are directly related to the Kirk effect.

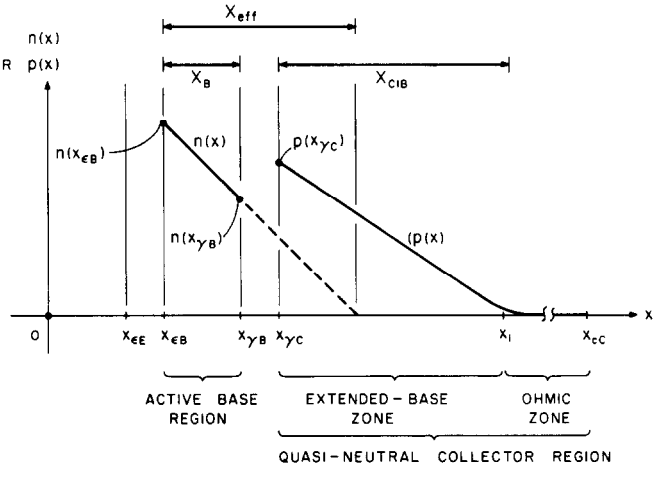

Fig. 9. The effective base thickness X_{eff} of the n^+pn^- transistor for d.c. calculations.

The term *Kirk effect* is currently used to describe behavior that results from the formation of an "extended base" zone. This zone, which is shown in Fig. 9, is a quasi-neutral region where the carrier concentrations greatly exceed their respective equilibrium values. Bowler and Lindholm[26] have shown that the Kirk effect can arise in two different ways. If the collector-base voltage V_{CB} is greater than a certain voltage V_{crit} (see Fig. 2), then the Kirk effect is related to one-dimensional behavior that is associated with space-charge-limited electron flow. This behavior and the closely related two-dimensional behavior described by van der Ziel and Agouridis[27] are not considered in this paper. If $0 < V_{CB} < V_{\text{crit}}$, then the Kirk effect is associated with behavior in the quasi-saturation regime.

In his paper, Kirk suggested that the effective base thickness X_{eff} of a n^+pn^- transistor is approximately equal to the sum of the active base thickness X_B and the extended base thickness X_{CIB}. For the n^+pn^- transistor considered here, this suggestion is not valid as Fig. 9 indicates. However, if the active base thickness were much greater and if the base-doping-concentration profile were Gaussian, then Kirk's suggestion would be much more accurate than Fig. 9 indicates. In other words, Kirk's suggestion is valid approximately for an epitaxial bipolar transistor in which the active base thickness is relatively large (>0.5 μm).

Gummel and Poon employed Kirk's suggestion in their "integral" charge control model. In fact, they wrote Gummel's relation, not in the extended form given here as eqn (75), but in a form which is more closely related to the following equation:

$$I_C = \frac{(qA_E n_i)^2 D_{nB}}{Q_{B0} + \dfrac{X_{\text{eff}}^2}{4D_{nB}} I_C} \exp \frac{q(-V_{EB})}{kT} \tag{96}$$

where $X_{\text{eff}} = X_B + X_{\text{CIB}}$. For many thin-base transistors, eqn (75) appears to be more accurate than eqn (96).

The equations for the n^+pn^- transistor can be converted to equations for an n^+pn^+ transistor if N_{DC} is made much larger than N_{AB}. For this condition, $n(x_{\gamma B})$ and Q_C^* can be set equal to zero so that eqn (74) becomes

$$I_C = \frac{(qA_E n_i)^2 \xi_1 D_{nB} \left[\exp \dfrac{q(-V_{EB})}{kT}\right]}{Q_{B0} + Q_B^* \left[\dfrac{\xi_1}{\xi_1^*} 2\right]} \tag{97}$$

and eqns (60) and (67) combine to give

$$Q_B^* = \frac{X_B^2}{2\xi_1 D_{nB}} \left(\frac{\xi_1^*}{\xi_1}\right) I_C. \tag{98}$$

Substituting this equation into eqn (97) yields

$$I_C = \frac{(qA_E n_i)^2 (\xi_1 D_{nB})}{Q_{B0} + \dfrac{X_B^2}{\xi_1 D_{nB}} I_C} \left[\exp \frac{q(-V_{EB})}{kT}\right] \tag{99}$$

which resembles Gummel's relation as given as eqn (96) since $X_{\text{eff}} = X_B$ for the given conditions.

Equation (99) describes the Webster effect in an n^+pn^+ transistor. For low currents, this equation becomes

$$I_C = qA_E \frac{D_{nB}}{X_B} \frac{n_i^2}{N_{AB}} \exp \frac{q(-V_{EB})}{kT} \tag{100}$$

since $Q_{B0} = qA_E N_{AB} X_B$. Equation (100) is consistent with the Ebers–Moll model. For high currents, eqn (99) becomes

$$I_C = qA_E \frac{2D_{nB}}{X_B} n_i \left[\exp \frac{q(-V_{EB})}{2kT}\right] \tag{101}$$

This equation can be obtained from eqn (100) by the replacement of (1) D_{nB} by $2D_{nB}$, (2) n_i^2/N_{AB} by n_i and (3) V_{EB} by $(1/2)V_{EB}$. Note that the first two replacements correspond to effects that can be "beneficial" and that the last replacement corresponds to an effect that is normally detrimental. The term *Webster effect* is usually associated with the detrimental effect.

For the n^+pn^- transistor, the Webster effect and the Kirk effect are always interrelated. At high currents, the Webster effect is typically less important than the Kirk effect. This suggests that the primary features of the Kirk effect can be found by setting $Q_B^* = 0$ even though this condition can never be realized. With $Q_B^* = 0$, eqn (74) becomes

$$I_C = \frac{(qA_E n_i)^2 \xi_1 D_{nB} \left[\exp \dfrac{q(-V_{EB})}{kT}\right]}{Q_{B0} + Q_C^* \left[\xi_2 \dfrac{\xi_2^*}{\xi_3} \dfrac{D_{nB}}{D_{nC}}\right]}. \tag{102}$$

This equation can be put in an interesting form as follows: Equation (40) is rewritten as

$$p(x_{\gamma C}) = \frac{N_{DC}}{2} \left\{ \frac{X_C I_C}{qA_E D_{nC} N_{DC}} - \frac{q(V_{CB} - V_{jC})}{kT} \right\}. \tag{103}$$

This equation is substituted in eqn (68) to give

$$Q_C^* = \frac{X_C^2}{4D_{nC}} I_C \left[1 - \frac{I_0^*}{I_C}\right]^2 \left(\frac{2}{\xi_3^*}\right) \tag{104}$$

in which I_0^* is defined as

$$I_0^* \doteq q\mu_{nC} N_{DC} \frac{A_E}{X_C} [V_{CB} - V_{jC}]. \tag{105}$$

Substitution of eqn (104) into eqn (102) gives

$$I_C = \frac{(qA_E n_i)^2 \xi_1 D_{nB} \left[\exp \dfrac{q(-V_{EB})}{kT}\right]}{Q_{B0} + \dfrac{X_C^2}{4D_{nC}} I_C \left[1 - \dfrac{I_0^*}{I_C}\right]^2 \left\{\xi_2 \dfrac{2}{\xi_3} \dfrac{D_{nB}}{D_{nC}}\right\}}. \tag{106}$$

If the factor in the brace were equal to unity and if V_{jC} were equal to a certain built-in voltage ψ_0, the eqn (106) would resemble an equation used by Rey and Bailbe[28] [see their eqn (42)]. Moreover, eqn (106) would also be consistent with an equation derived by Hower[29]. For high values of I_C, both forms of Gummel's relation given here [eqns (75) and (96)] approximate eqn (106).

8. SOME ADDITIONAL IDEAS IMPORTANT TO THE DERIVATION

In the derivation of the n^+pn^- transistor model, high-current effects in the emitter region are assumed to be negligible. Because $N_{DE} \gg N_{AB}$, this assumption is well justified for d.c. current-gain values greater than unity. The model can be extended to describe analytically such effects in cases where recombination may be neglected in the emitter region ($X_E \ll L_{pE}$).

The graded-base transistor is not considered in this paper because analytical solutions are out of reach for typical transistors[30, 31]. However, it should be noted that the Fletcher boundary conditions can be extended analytically for graded junctions (e.g. see Hauser[16]).

In the active base region, potential differences in the x-direction can be calculated by integrating the electric field. Equation (18) shows that the electric field consists of an ohmic part and an ambipolar-diffusion part. In the quasi-neutral collector region, the corresponding calculation involves eqn (33), which can also be divided into ohmic and ambipolar-diffusion parts. For high-frequency a.c. calculations, this division may be required.

It is a good approximation to set the x component of $\vec{J}_p(x, y)$ equal to zero in the active base region. The corresponding approximation can not be made in the quasi-neutral collector region.

The variable γ_C is introduced to account for minority carrier flow in the collector region. If an ohmic zone exists in the collector region, then γ_C is approximately equal to $n_i^2/(b_C N_{DC}^2)$. But a more accurate value of γ_C is required for several equations. Consider eqn (9) which is approximately equivalent to the following equation if the transistor is operating in the quasi-saturation regime:

$$(V_{CB} - V_{jC}) = \frac{kT}{q} \ln \left[\frac{p(x_{\gamma C})/N_{DC}}{(n_i/N_{DC})^2 - \gamma_C b_C} \right]. \quad (107)$$

For the numerical values given in Table 3, eqn (107) is valid only if $\gamma_C = n_i^2/(b_C N_{DC}^2) - 3.68 \times 10^{-45}$. If γ_C were equal to zero (i.e. if J_{pC} were equal to zero), then the right-hand side of eqn (107) would be approximately equal to $-V_{jC}$, and hence much less than $(V_{CB} - V_{jC})$. If γ_C were to approach $n_i^2/(b_C N_{DC}^2)$, the the right-hand side of eqn (107) would diverge, and hence could not equal $(V_{CB} - V_{jC})$. Thus the seemingly negligible term (3.68×10^{-45}) is of crucial importance for calculating some quantities (not including terminal I–V characteristics).

Equation (107) can be put into the following form

$$(V_{CB} - V_{jC}) = V_{CIB} + V_{\text{ohmic}} \quad (108)$$

where

$$V_{CIB} = \frac{kT}{q} \ln \frac{p(x_{\gamma C})}{n_i} \quad (109)$$

$$V_{\text{ohmic}} = \frac{kT}{q} \ln \left[\frac{(N_{DC}/n_i)}{1 - \gamma_C b_C (N_{DC}/n_i)^2} \right]. \quad (110)$$

If the boundary x_i between the extended base zone and the ohmic zone is defined by the condition $p(x_i) = n_i$, then eqns (109) and (110) give approximately the potential differences across these two zones. Since V_{jC} is approximately $-(kT/q) \ln [p(x_{\gamma C}) N_{DC}/n_i^2]$, eqn (108) reduces to

$$V_{CB} = V_{\text{ohmic}} - \frac{kT}{q} \ln \frac{N_{DC}}{n_i}. \quad (111)$$

This equation shows that V_{ohmic} is approximately equal to the applied collector-base voltage V_{CB}. Moreover, it shows that V_{jC} is nearly independent of V_{CB}. (V_{jC} is primarily dependent upon current I_C.) In other words, voltage changes across the collector-base space-charge region are cancelled by the voltage changes across the extended base region.

At high currents, eqn (7) can be written as

$$(V_{EB} - V_{jE}) = -\frac{kT}{q} \ln \frac{n(x_{\epsilon B})}{N_{AB}}. \quad (112)$$

Since V_{jE} is about equal to $-(kT/q) \ln [n(x_{\epsilon B}) N_{AB}/n_i^2]$, eqn (112) becomes

$$(V_{EB}/2) = V_{jE} - \frac{kT}{q} \ln \frac{N_{AB}}{n_i}. \quad (113)$$

This equation shows that V_{jE} is approximately equal to $(V_{EB}/2)$, which is the high-current result obtained by Webster. Note that the constant terms in eqns (111) and (113) are not equal to equilibrium junction voltages.

Equations (1) through (9) of the n^+pn^- transistor model are inaccurate for equilibrium conditions. If such conditions are important, one can employ the more general equations given in the derivation immediately prior to each of the final form eqns (1)–(9) of the model.

The n^+pn^- transistor can be characterized by the ratio

$$R = \frac{N_{AB} X_B / D_{nB}}{N_{DC} X_C / D_{nC}}. \quad (114)$$

This ratio appears, for example, in eqn (55). For very large N_{DC}, the transistor reverts to the n^+pn^+ structure.

While the equations constituting the abridged model, eqns (35)–(43), may still seem comparatively complex, their use for quantitative calculations is straightforward and comparatively easy. All computations in this paper (such as those for Figs. 5 and 6) were carried out using an HP-25 calculator.

9. THE $n^+pn^-n^+$ TRANSISTOR MODEL

The $n^+pn^-n^+$ transistor is assumed to have a structure that is identical to the n^+pn^- structure already given except that the ohmic contact region is replaced by a very thick n^+-substrate region. As shown in Fig. 10, this structural modification introduces a high-low space-

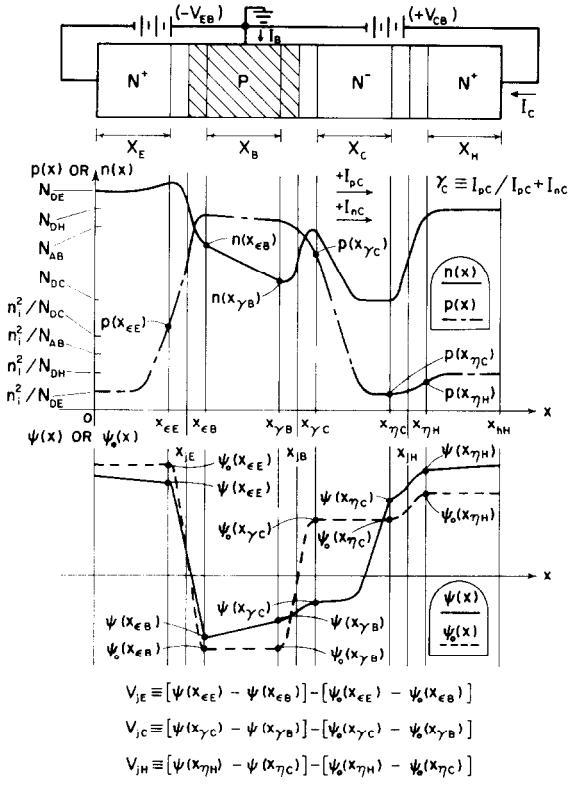

Fig. 10. The fourteen variables of the $n^+pn^-n^+$ transistor model. Many features of this figure are identical to those of Fig. 1.

and

$$V_{CB} = V_{jC} + V_{jH} + \frac{kT}{q}\left[\frac{1+\gamma_C(b_C-1)}{1-\gamma_C(b_C+1)}\right] \ln\left[\frac{p(x_{\gamma C})[1-\gamma_C(b_C+1)]-\gamma_C b_C N_{DC}}{p(x_{\eta C})[1-\gamma_C(b_C+1)]-\gamma_C b_C N_{DC}}\right]. \quad (116)$$

The first of the three new equations gives an expression for the hole current $\gamma_C I_C$ consisting of holes that are emitted from the substrate region if $V_{CB} > 0$. This equation is

$$\gamma_C I_C = -qA_E \frac{D_{pH}}{L_{pH}}[p(x_{\eta H}) - (n_i^2/N_{DH})] \quad (117)$$

Finally, the last two equations of the model for the $n^+pn^-n^+$ transistor are

$$p(x_{\eta C}) = N_{DC}\left\{\left[\exp\frac{q(-V_{jH})}{kT}\right]-1\right\} \quad (118)$$

$$p(x_{\eta H}) = \frac{N_{DC}^2}{N_{DH}}\left[\exp\frac{q(-V_{jH})}{kT}\right]\left\{\left[\exp\frac{q(-V_{jH})}{kT}\right]-1\right\}. \quad (119)$$

These two equations can be derived from the Fletcher boundary conditions for a pn diode by the following procedure: The Fletcher boundary conditions for the hole concentrations at the two boundaries of a pn space-charge region are given by

$$p(x_{\mu P}) = \frac{(p_{0P}-n_{0P})n_{0N}p_{0P} + (n_{0N}-p_{0N})n_{0P}p_{0P}\left[\exp\frac{q(-V_j)}{kT}\right]}{p_{0P}n_{0N} - n_{0P}p_{0N}\left[\exp\frac{q(-V_j)}{kT}\right]^2} \quad (120)$$

$$p(x_{\mu N}) = \frac{(p_{0P}-n_{0P})p_{0N}n_{0N}\left[\exp\frac{q(-V_j)}{kT}\right] + n_{0P}p_{0N}(n_{0N}-p_{0N})\left[\exp\frac{q(-V_j)}{kT}\right]^2}{p_{0P}n_{0N} - n_{0P}p_{0N}\left[\exp\frac{q(-V_j)}{kT}\right]^2}. \quad (121)$$

charge region and a quasi-neutral heavily-doped region in which recombination of carriers is important (i.e. $L_{pH} \ll X_H$). Three new internal variables are also introduced: $p(x_{\eta C})$, $p(x_{\eta H})$ and V_{jH}. The first two variables represent the minority carrier concentrations at the locations $x_{\eta C}$ and $x_{\eta H}$. The last variable is defined as the potential drop across the high-low space-charge region minus the corresponding drop for equilibrium conditions. The model for the $n^+pn^-n^+$ transistor consists of eqns (1)–(7), modifications of eqns (8) and (9), and three new equations. The two modified equations are obtained from eqns (8) and (9) by the replacement of n_i^2/N_{DC} by $p(x_{\eta C})$ and by the replacement of V_{jC} with $V_{jC} + V_{jH}$. The resulting equations are

By the substitution of the notation given in row two of Table 4 and by the use of the approximations given in Table 5, eqns (118) and (119) result directly from eqns (120) and (121).

Typical hole- and electron-concentration profiles for the $n^+pn^-n^+$ transistor are shown in Fig. 11. Moreover, the corresponding profiles for the n^+pn^- transistor are given on the same diagram. The vertical scale of Fig. 11 is logarithmic, and the profiles for the n^+pn^- transistor correspond directly with those given in Fig. 6. Because the high-low junction represents a barrier to minority carriers, the hole current through the collector region of the $n^+pn^-n^+$ transistor is much smaller than the corresponding current in the n^+pn^- transistor operating

$$I_C = \frac{qA_E D_{nC}}{[1-\gamma_C(b_C+1)]X_C}\left\{2[p(x_{\gamma C}) - p(x_{\eta C})] + N_{DC}\left[\frac{1+\gamma_C(b_C-1)}{1-\gamma_C(b_C+1)}\right]\ln\left[\frac{p(x_{\gamma C})[1-\gamma_C(b_C+1)]-\gamma_C b_C N_{DC}}{p(x_{\eta C})[1-\gamma_C(b_C+1)]-\gamma_C b_C N_{DC}}\right]\right\} \quad (115)$$

Table 4. Notation for pn junction and for the high-low junction of an $n^+pn^-n^+$ transistor

pn DIODE SPACE-CHARGE REGION	$p(x_{\mu P})$	$p(x_{\mu N})$	$(-V_j)$	n_{OP}	p_{OP}	n_{ON}	p_{ON}
HIGH-LOW SPACE-CHARGE REGION	$p(x_{\eta C})$	$p(x_{\eta H})$	$(-V_{jH})$	n_{OC}	p_{OC}	n_{OH}	p_{OH}
VAN VLIET'S NOTATION	p_i^*	p_i	V	n_o^*	p_o^*	n_o	p_o

Table 5. Additional approximation for the $n^+pn^-n^+$ transistor†

$N_{DC} >> n_i$	$N_{DH} >> n_i$	GROUP A
$X_C << L_{pC}$	$X_H >> L_{pH}$	
$n_{OC} \approx N_{DC}$	$n_{OH} \approx N_{DH}$	GROUP B
$p_{OC} \approx \frac{n_i^2}{N_{DC}}$	$p_{OH} \approx \frac{n_i^2}{N_{DH}}$	
$N_{OH} >> N_{DC}$	$1 >> \left[\frac{N_{DC}}{N_{DH}}\right]^2 \left[\exp \frac{q(-V_{jH})}{kT}\right]^2$	GROUP C

†Groups A, B and C are similar to the corresponding Groups of Table 2.

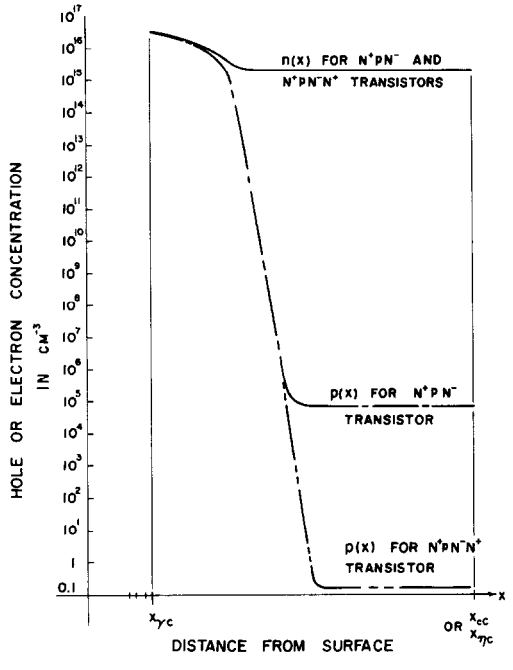

Fig. 11. The hole and electron profiles of an $n^+pn^-n^+$ transistor compared with those of an n^+pn^- transistor. The profiles for the n^+pn^- transistor correspond to those given in Fig. 6.

under the same external bias conditions. Thus, by the replacement of the ohmic contact region by the thick substrate region, the assumptions that were used to derive eqns (5)–(7) become more accurate.

The $n^+pn^-n^+$ transistor model as given by eqns (1)–(7) and eqns (115)–(119) employs the Fletcher boundary conditions. An exactly equivalent model employing the Misawa boundary conditions[32] can be derived as follows. The Misawa variables are defined as:

$$\Delta\phi_{jE} = \phi_n(x_{\epsilon E}) - \phi_p(x_{\epsilon B}) \tag{122}$$

$$\Delta\phi_{jC} = \phi_n(x_{\gamma C}) - \phi_p(x_{\gamma B}) \tag{123}$$

$$\Delta\phi_{jH} = \phi_n(x_{\eta H}) - \phi_p(x_{\eta C}). \tag{124}$$

To transform from the Fletcher variables (V_{jE}, V_{jC} and V_{jH}) to the Misawa variables ($\Delta\phi_{jE}$, $\Delta\phi_{jC}$ and $\Delta\phi_{jH}$), we introduce the following three equations:

$$(-\Delta\phi_{jE}) = (-V_{jE}) + \frac{kT}{q}\ln\left[\frac{p(x_{\epsilon E}) + (n_{0E} - p_{0E})}{n_{0E}}\right] + \frac{kT}{q}\ln\left[\frac{n(x_{\epsilon B}) + (p_{0B} - n_{0B})}{p_{0B}}\right] \tag{125}$$

$$(-\Delta\phi_{jC}) = (-V_{jC}) + \frac{kT}{q}\ln\left[\frac{p(x_{\gamma C}) + (n_{0C} - p_{0C})}{n_{0C}}\right] + \frac{kT}{q}\ln\left[\frac{n(x_{\gamma B}) + (p_{0B} - n_{0B})}{p_{0B}}\right] \tag{126}$$

$$(-\Delta\phi_{jH}) = (-V_{jH}) + \frac{kT}{q}\ln\left[\frac{p(x_{\eta H}) + (n_{0H} - p_{0H})}{n_{0H}}\right] + \frac{kT}{q}\ln\left[\frac{p(x_{\eta C}}{p_{0C}}\right]. \tag{127}$$

Each of these equations is related to a pn-diode equation given by van Vliet[7] (his eqn 32a). Nussbaum[14] has given a complete discussion on the validity of such equations. With eqns (125)–(127), the $n^+pn^-n^+$ transistor model as already given can be transformed into the following twelve equations:

$$p(x_{\epsilon E})N_{DE} = n_{iE}^2 \exp\left[\frac{q(-\Delta\phi_{jE})}{kT}\right] \tag{128}$$

$$n(x_{\epsilon B})[n(x_{\epsilon B}) + N_{AB}] = n_i^2 \exp\left[\frac{q(-\Delta\phi_{jE})}{kT}\right] \tag{129}$$

$$n(x_{\gamma B})[n(x_{\gamma B}) + N_{AB}] = n_i^2 \exp\left[\frac{q(-\Delta\phi_{jC})}{kT}\right] \tag{130}$$

$$p(x_{\gamma C})[p(x_{\gamma C}) + N_{DC}] = n_i^2 \exp\left[\frac{q(-\Delta\phi_{jC})}{kT}\right] \tag{131}$$

$$I_B + \gamma_C I_C = qA_E \frac{D_{pE}}{L_{pE}}\left[p(x_{\gamma E}) - \frac{n_{iE}^2}{N_{DE}}\right] \tag{132}$$

$$I_C(1-\gamma_C) = qA_E \frac{D_{nB}}{X_B}\left\{2[n(x_{\epsilon B}) - n(x_{\gamma B})] - N_{AB}\ln\left[\frac{n(x_{\epsilon B}) + N_{AB}}{n(x_{\gamma B}) + N_{AB}}\right]\right\} \tag{133}$$

$$V_{EB} = \Delta\phi_{jE} \tag{134}$$

$$I_C = qA_E \frac{D_{nC}}{X_C}\frac{1}{[1-\gamma_C(b_C+1)]}\left\{2[p(x_{\gamma C}) - p(x_{\eta C})] + N_{DC}\left[\frac{1+\gamma_C(b_C-1)}{1-\gamma_C(b_C+1)}\right]\ln\left[\frac{p(x_{\gamma C})[1-\gamma_C(b_C+1)] - \gamma_C b_C N_{DC}}{p(x_{\eta C})[1-\gamma_C(b_C+1)] - \gamma_C b_C N_{DC}}\right]\right\} \tag{135}$$

$$V_{CB} = \frac{kT}{q}\left[\frac{1+\gamma_C(b_C-1)}{1-\gamma_C(b_C+1)}\right]\ln\left[\frac{p(x_{\gamma C})[1-\gamma_C(b_C+1)]-\gamma_C b_C N_{DC}}{p(x_{\eta C})[1-\gamma_C(b_C+1)]-\gamma_C b_C N_{DC}}\right]$$
$$+\Delta\phi_{jC}+\frac{kT}{q}\ln\left[1+\frac{p(x_{\gamma C})}{N_{DC}}\right]+\Delta\phi_{jH}+\frac{kT}{q}\ln\left[\frac{p(x_{\eta C})}{n_i^2/N_{DC}}\right] \quad (136)$$

$$\gamma_C I_C = -qA_E\frac{D_{pH}}{L_{pH}}\left[p(x_{\eta H})-\frac{n_i^2}{N_{DH}}\right] \quad (137)$$

$$p(x_{\eta C})[p(x_{\eta C})+N_{DC}] = n_i^2\exp\left[\frac{q(-\Delta\phi_{jH})}{kT}\right] \quad (138)$$

$$p(x_{\eta H})N_{DH} = n_i^2\exp\left[\frac{q(-\Delta\phi_{jH})}{kT}\right]. \quad (139)$$

10. CONCLUSIONS

The $n^+pn^-n^+$ transistor model as just given can be used to predict the characteristics of not only the epitaxial transistor but also the low-emitter-impurity-concentration (LEC) transistor[33] and the integrated-injection-logic (I^2L) transistor[34, 35]. The predicted characteristics for the last two transistors will be described in subsequent papers. The predicted characteristics for the epitaxial transistor have been described here. These characteristics demonstrate that (1) Kirk's suggestion is not always valid and (2) Gummel's relation for the n^+pn^+ transistor can not be simply extended for the $n^+pn^-n^+$ transistor. These statements are illuminated by the following sequence of ideas.

The minority-carrier-concentration profile in the active base region is nearly a straight line under *all* operating conditions, just as in the simplest model of bipolar transistor operation. This profile has a negative slope at every point when $I_C > 0$; it has a positive slope when $I_C < 0$. Forward operation ($I_C > 0$) comprises three regimes: (a) The forward-saturation regime, where forward bias is applied across both the emitter-base and the collector-base terminal pairs, (b) The quasi-saturation regime, where the collector-base terminals receive a reverse bias, but because of ohmic drop in the collector region, the collector-base junction is forward biased internally, (c) The forward-active regime. In the quasi-saturation regime, the quasi-neutral collector region is divisible into an extended base zone adjacent to the collector-base space-charge region and an ohmic zone adjacent to the high-low space-charge region; the slopes of the electron-concentration profiles at every point in the active base region and the extended base zone of the collector region never differ by more than a factor of two. The initial sharp decline of current gain β_F with increasing I_C (or I_B) in the quasi-saturation regime occurs because the electron concentration at the base boundary of the collector-base space-charge region increases approximately as the square of the hole concentration at the collector boundary of this region. The effective base thickness is always less than the sum of the active base thickness and the extended base thickness because of a significant "vertical step" in the electron-concentration profile located near the metallurgical collector-base junction. This step becomes small at extreme currents where current gain β_F is too low to be practically interesting.

The $n^+pn^-n^+$ transistor model differs from existing models in two ways. First, the ambipolar approach is used for the quasi-neutral collector region. Second, the Fletcher boundary conditions or the Misawa boundary conditions are employed for the collector-base and high-low space-charge regions. A necessary element in using the ambipolar approach is the injection variable γ_C, defined as the ratio of the hole current $I_p(x_{\gamma C})$ to the total current $I(x_{\gamma C})$. All previous theories have assumed that γ_C has a constant value equal to zero or $n_i^2/(b_C N_{\gamma C}^2)$. Both of these values lead to theoretical contradictions. A necessary condition for employing the Fletcher boundary conditions is eqn (116). This equation results from the ambipolar approach; it gives a relation connecting the two junction voltages V_{jC} and V_{jH} with the collector-base (terminal) voltage V_{CB}. A necessary condition for employing the Misawa boundary conditions is eqn (136). This equation also results from the ambipolar approach; it gives a relation connecting the two potential differences $\Delta\phi_{jC}$ and $\Delta\phi_{jH}$ with the collector-base (terminal) voltage V_{CB}.

For all but high-frequency calculations (which are not discussed here) the analytical $n^+pn^-n^+$ transistor model given above is simpler, easier to use, and more accurate than a corresponding charge-control model.

Acknowledgement—The authors are indebted to four persons—Profs. Nussbaum and van der Ziel of the University of Minnesota, Prof. van Vliet of the University of Montreal and Dr. Gummel of Bell Laboratories—for reviewing critically a preliminary copy of this paper. Financial support that made this work possible was provided by the National Science Foundation through Grant GK 39890 and also by the Graduate School of the University of Minnesota.

REFERENCES

1. J. J. Ebers and J. L. Moll, *Proc. IRE* **42**, 1761 (1954).
2. H. K. Gummel and H. C. Poon, *Bell. Syst. Tech. J.* **49**, 827 (1970).
3. C. T. Kirk, Jr., *IRE Trans. Electron Dev.* **ED-9**, 164 (1962).
4. W. M. Webster, *Proc. IRE* **42**, 914 (1954).
5. N. H. Fletcher, *J. Electron.* **2**, 609 (1957).
6. W. van Roosbroeck, *Phys. Rev.* **91**, 282 (1953).
7. K. M. van Vliet, *Solid-St. Electron.* **9**, 185 (1966).
8. K. M. van Vliet and H. S. Min, *Solid-St. Electron.* **17**, 267 (1974).
9. J. R. A. Beale and J. A. G. Slatter, *Solid-St. Electron.* **11**, 241 (1968).
10. J. A. Pals and H. C. de Graaff, *Philips Res. Repts* **24**, 53 (1969).
11. H. K. Gummel, *Solid-St. Electron.* **10**, 209 (1967).
12. S. Hazman, *Solid-St. Electron.* **10**, 269 (1967).
13. K. M. van Vliet, *Solid-St. Electron.* **10**, 263 (1967).
14. A. Nussbaum, *Solid-St. Electron.* **12**, 177 (1969).

15. H. D. Barber, *Solid-St. Electron.* **12**, 425 (1969).
16. J. R. Hauser, *Solid-St. Electron.* **14**, 133 (1971).
17. A. van der Ziel, *Solid-St. Electron.* **16**, 1509 (1973).
18. A. Nussbaum, *Solid-St. Electron.* **18**, 107 (1975).
19. H. J. J. de Man, *IEEE Trans. Electron. Dev.* **ED-18**, 833 (1971).
20. R. P. Mertens, H. J. de Man and R. J. von Overstraeten, *IEEE Trans. Electron. Dev.* **ED-20**, 772 (1973).
21. E. S. Rittner, *Phys. Rev.* **94**, 1161 (1954).
22. H. K. Gummel, *Proc. IEEE* **49**, 834 (1961).
23. H. K. Gummel, *Bell System Tech. J.* **49**, 115 (1970).
24. J. P. McKelvey, *Solid State And Semiconductor Physics.* Harper and Row, New York (1966).
25. J. M. Early, *Proc. IRE* **40**, 1401 (1952).
26. D. L. Bowler and F. A. Lindholm, *IEEE Trans. Electron. Dev.* **ED-20**, 257 (1973).
27. A. van der Ziel and D. Agouridis, *Proc. IEEE* **54**, 411 (1966).
28. G. Rey and J. P. Bailbe, *Solid-St. Electron.* **17**, 1045 (1974).
29. P. L. Hower, *IEEE Trans. Electron. Dev.* **ED-20**, 426 (1973).
30. M. B. Das and A. R. Boothroyd, *IRE Trans. Electron. Dev.* **ED-8**, 15 (1961).
31. J. Lindmayer and C. Wrigley, *Solid-St. Electron.* **2**, 79 (1961).
32. T. Misawa, *J. Phys. Soc. Japan* **11**, 728 (1956).
33. H. Yagi and T. Tsuyuki, Supplement to *J. Japan Soc. Appl. Phys.* **44**, 279 (1975).
34. H. H. Berger and S. K. Wiedmann, *IEEE J. Solid-St. Cir.* **SC-7**, 340 (1972).
35. K. Hart and A. Slob, *IEEE J. Solid-St. Cir.* **SC-7**, 346 (1972).